Proceedings World Geothermal Congress 2020+1
Reykjavik, Iceland, April - October 2021

Analysis of Well Testing, Temperature and Pressure in High Temperature Wells of Aluto Langano, Ethiopia

Mesay Fekadu Biru

Ethiopian Electric Power (EEP)

Ethiopia

abushmech@gmail.com

Keywords: Well testing, temperature, pressure, Aluto Langano, conceptual modelling

ABSTRACT

Drilling in the Aluto-Langano geothermal field started in 1981 intending to harness steam for electric power production. Eight exploration wells were drilled between 1981 and 1986, with four productive, one reinjection and three non-productive wells. Recently, between 2013 and 2015, two-directional wells were drilled, and they are still undergoing different measurements and tests. Measurements from these wells, LA-9D and LA-10D, as well as from an older one, LA-3, were analysed and are presented in the report. Results from analyses of injection tests for wells LA-3 and LA-10D are characterized by having fairly good transmissivity and storativity values and the injectivity indices are rather low. The evaluated fluid enthalpy for wells LA 9D and LA-10D is in the range of 1600-2200 kJ/kg, with steam flow ranging from 5-9 kg/s with separation pressure of 1 bar-a as well as with separation pressure of 5 bar-a of Aluto-Langano pilot power plant.

Formation temperatures of wells LA-9D and LA-10D were estimated by extrapolation of temperature logs from their warm-up periods. The results suggest that the reservoir temperature is in the range of 300-315°C and reservoir pressure in the range of 85 100 bar for both wells.

1. INTRODUCTION

Ethiopia is one of the East African countries with the most significant geothermal resources. Exploration of the resources started in 1969, and they are gradually being investigated. A total of 10 wells have already been drilled in one of the most promising fields, the Aluto Langano geothermal field, but it has not yet been utilized except to a little extent. In this report, the results of analyses conducted on measurements from the Aluto-Langano geothermal field are introduced. From this area, wells LA-3, LA-9D and LA-10D were selected for the study. Different types of analyses were performed including simulations of injection tests from the end of drilling of LA-3 and LA-10D, as well as estimation of formation temperature, initial pressure and analysis of discharge testing from directionally drilled wells, LA-9D and LA-10D.

The injection test simulation was made by using Welltester software based on non-linear regression (Júlíusson et al., 2008, Marteinsson, personal communication in August 2016). The injectivity index is the first parameter analysed and is a simple relationship between change inflow and change in pressure, reflecting the capacity of a well or how open it is to the surroundings, which is useful for determining whether a well is sufficiently open to be a successful producer, if it should be stimulated or if drilling should possibly be continued to look for deeper, better feed zones.

Formation temperature estimation was obtained by using the Berghiti software developed at ISOR (Helgason, 1993, Marteinsson, personal communication in August 2016). Formation temperature estimation is important to increase the knowledge about a geothermal system for decision making when selecting new sites and in developing conceptual models. The initial pressure is also obtained by using Predyp from ICEBOX software (Arason et al., 2004). Discharge test analysis is obtained by using Lip from ICEBOX software.

Discharge data from LA-9D and LA 10D were analysed at different wellhead pressures. A short description of Aluto Langano geothermal system in Chapter 2. Injection tests from two wells were analysed and discussed in Chapter 3. Temperature and pressure profiles during the warm-up period were analysed to determine the formation temperature and initial pressure and the process and results are introduced in Chapter 4, and finally, the result of discharge testing will be analysed followed by discussion and conclusion in Chapters 5 and 6.

1.1 Geothermal System

Geothermal resources are distributed throughout the planet. Even though most geothermal systems and the greatest concentration of geothermal energy are associated with the Earth ‘s plate boundaries, geothermal energy may be found in most countries. It is highly concentrated in volcanic regions, but also be found as warm groundwater in sedimentary formations worldwide as low-temperature systems (Axelsson, 2012). Geothermal systems are governed by the surface and subsurface hydrological pattern, heat source and surface activity associated with a geothermal resource. While the geothermal field is considered to refer to the area of geothermal activity on the surface, intended as a geographic description, it is regarded as a component of the geothermal system. The geothermal reservoir is the section in the geothermal system that can be economically exploited for energy utilisation.

Geothermal systems exist in different forms and are classified on the basis of reservoir temperature, enthalpy, physical state, geological settings and its nature (Axelsson, 2012). Low-temperature systems (< 150°C), are also referred to as low-enthalpy systems (<800 KJ/kg). This type of geothermal systems exists in sedimentary basins with permeability at great depth and classified

as liquid dominated geothermal systems. High-temperature systems (> 200°C) may also be described as high enthalpy systems (>800 kJ/kg). These are mostly characterized by active volcanism, the heat source being shallow magma, intrusions or dykes.

1.2 Geothermal Wells

Geothermal wells play a key role in the research and development of geothermal systems. Geothermal wells provide access to for direct testing and measurements into the systems. They are vital components in both geothermal research and utilisation since they provide essential access for both energy extraction and information collection (Axelsson, 2013). Geothermal wells can be classified as low temperature and high-temperature wells. A low temperature (liquid dominated) well produces liquid water at wellhead while, high temperature well in which the flow from feed zone(s) is liquid or two-phase produces either a two-phase or dry steam at the wellhead (Grant and Bixely, 2011).

There are many types of geothermal wells; some of them are described as follows. Temperature gradient wells are designed as slim and shallow, typically less than 100 m in depth, drilled in the early stage of geothermal research. Their main purpose is to determine the temperature gradient near the surface at shallow depth. Another type is the exploration wells which are drilled during the exploration phase, usually deeper than gradient wells to hit the geothermal reservoir with the purpose of exploring its conditions. The production wells have the main purpose of facilitating the geothermal energy extraction from the reservoir but are also used for gaining further information about the reservoir. The step-up wells are drilled to extend the confirmation of a particular geothermal reservoir while the make-up wells are used to make up for either damaged production wells due to scaling or collapse or regular declining output of production wells with time. The injection wells are used for injecting water back into the geothermal system which helps in increasing production capacity, for environmental management and decreasing pressure drops. The monitoring wells are used for management purposes, i.e. for monitoring how the geothermal system reacts to the production (Axelsson, 2013).

2. ALUTO-LANGANO GEOTHERMAL SYSTEM

2.1 Location and geological setting of Aluto-Langano

Ethiopia launched a long-term geothermal exploration in 1969. Over the years and one of the East African countries with the most significant geothermal resources. Over the years, a good inventory of the potential target areas has been built up, and more than 23 prospects are judged as having the potential for electricity production (Teklemariam, 1996).

The geothermal resources are present in the Main Ethiopian Rift System and in the Afar depression, which are parts of the Great East Africa Rift System. More than sixteen geothermal prospects are located along this rift that is believed to have the potential for electricity production. Aluto Langano, Tendaho, Corbetti, Abaya, Tulumoye-Gedemsa, Dofan and Fantale (Figure 1) are a few of the prospect areas in which detailed exploration study and drilling have started due to their expected potential and their strategic location relative to the national electric grid (Worku Sisay, 2016).

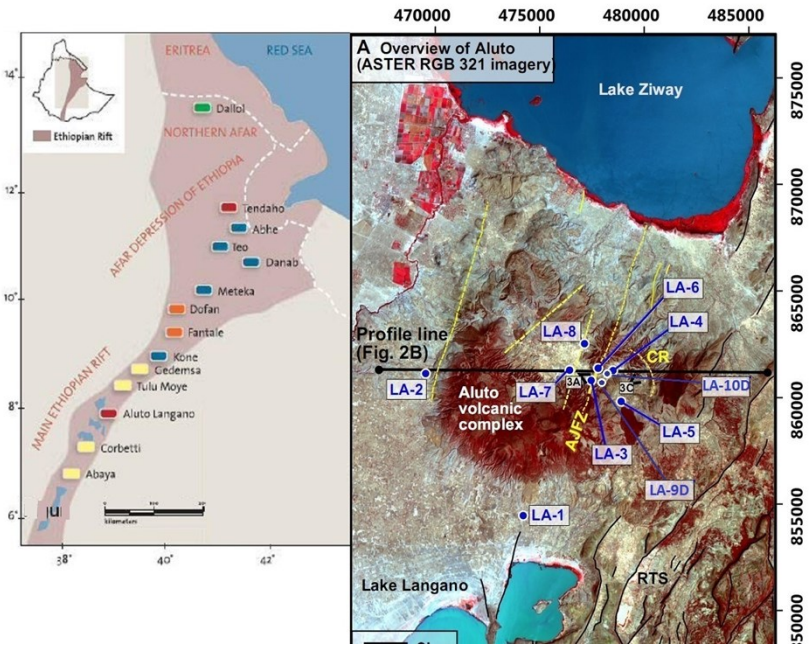

Figure 1: Main Ethiopian rift valley to the left and Aluto volcanic complex to the right (Hutchison et al., 2015)

2.2 Surface Geology of Aluto-Langano

Aluto volcanic complex covers an area of about 100 km^2 between lakes Langano and Ziway (Figures 1 and 2) and rises to an elevation of 690 m above the surrounding Adami-Tullu plain which has an elevation of about 1600 m a.s.l. The broad truncated base and a summit caldera are 6 km by 9 km (with an area of 37 km^2) elongated in a WNW direction have formed a basin of

internal drainage (Worku Sisay, 2016). Volcanic activity at the Aluto volcanic centre was entirely contained in the Quaternary with earlier sub-lacustrine eruptions. The activity initiated with a rhyolite dome building phase intervened by explosive pyroclastic pumice eruptions and a major caldera-forming pyroclastic eruption. The ignimbrite is now exposed on the flanks of the Aluto volcanic massif as pumices ignimbrites, and sub-aqueous pumices tuff with minor intercalations of lacustrine sediments. Post-caldera collapse rhyolite flows, domes with minor pyroclastic products formed along the NE-SE segment of the Aluto Caldera rim on a basement of pumices ignimbrites and older rhyolite. Predominantly rhyolite post-caldera lava and pyroclastic have erupted from numerous craters with all vents showing a clear control by either the caldera ring fracture or the NNE trending faults of the Wonji Fault Belt (WFB). The northern segment of the centre is characterised by large rhyolite domes and flows, which do not show a marked structural control. Minor basaltic lavas have erupted from the NNE trending faults east of Aluto massif. The Aluto caldera is covered by alluvial sediments (Teklemariam and Beyene, 2000).

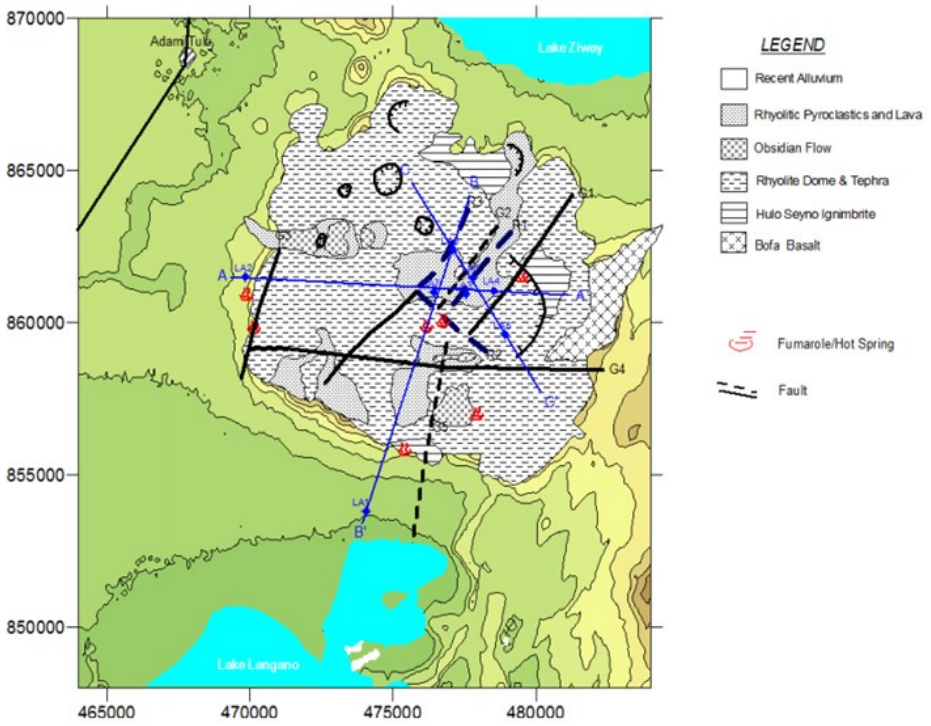

Figure 2: Geological map of Aluto-Langano geothermal field (William et al., 2015)

2.3 Exploration Drilling

Aluto Langano is the first geothermal field in Ethiopia to be exploited. In this area, eight deep exploration wells (LA-1 to LA-8) (Figure 3) were drilled in 1981 to 1986 with a maximum depth of 2500m, reaching temperature of up to 335°C (Teklemariam and Beyene, 2000). Wells LA-1 and LA-2 were drilled at the southern and western flanks of Aluto Volcanic Complex (AVC), respectively (Figure 3), and were characterised by low temperature and permeability. Wells LA-3 to LA-8 was sited on top of Aluto Langano in the south-eastern part of the area. LA-3 and LA-6 were drilled in the most active fault system, Wonji Fault Belt (WFB) (Figure 2), trending in NNE direction, and where maximum temperature recorded was 315°C and 335°C, respectively (UNDP, 1986). LA-4 and LA-5 were drilled in the eastern part of the Wonji Fault Belt and LA-7 and LA-8 in the western part (Figure 3).

The first 7.2MWe pilot power plant was installed in the Aluto Langano field by the Ethiopian Electric Power Corporation and connected to the national power grid in May 1998. It was started by connecting four production wells, LA-3, LA-4, LA-6 and LA-8, and with one reinjection well, LA-7 (Teklemariam and Beyene, 2000).

The expected capacity of this geothermal field was 30 MWe over for 30 years. The pilot power plant has not been in full operation due to problems related to the production wells (E.g. decline of well pressures, scaling and wellhead valve problems) and problems related to the power plant involving cooling tower fan breakdowns, Pentane leakage from the heat exchangers and so on. According to Kebede (2012), the plant has been partially renewed and started to produce 4MWe in 2007. Recently, two exploration wells have been drilled, LA 9D and LA-10D, with the use of a rig owned by the Geological Survey of Ethiopia. LA-9D and LA-10D are the first directional wells in Ethiopia, and both wells are in the testing phase.

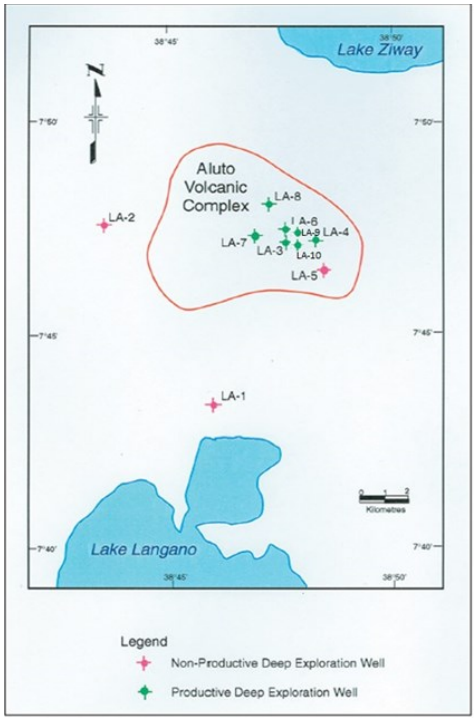

Figure 3: Wells LA-1 to LA-10D located in Aluto-Langano geothermal field

Information about wells LA-3 to LA-10D is in Table 1, where the status codes represent:

P: Productive

NP: Non-productive

RW: Reinjection well

Table 1: Information about exploration wells in Aluto-Langano geothermal field

Well	LA-3	LA-4	LA-5	LA-6	LA-7	LA-8	LA-9D	LA-10D
Drilled depth (m)	2114	2062	1867	2203	2448	2500	1921	1950
Elevation (m.a.s.l)	1921	1956	2037	1962	1891	1895	1963	1960
Permeable zones (m)	2000-2121	1445-1800	-	2000-2200	2100-2300	2300-2500	760-1350	920-1760
Maximum T (°C)	322	240	210	335	228	284	308	310
Status of the well	P	P	NP	P	RW	P	P	P
Year of drilling	21/1/83-13/6/83	6/783-23/10/83	15/11/83-11/3/84	24/3/84-2/7/84	12/7/84-21/10/84	26/10/84-13/5/84	12/11/13-01/02/15	25/06/15-02/10/15

3. INJECTION WELL TESTING

3.1 Introduction of Pressure Transient Analysis

Immediately after completion of geothermal well drilling, well testing is conducted in order to assess the conditions of a well and the properties of the reservoir intersected by the well, by subjecting it to injection or production. During an injection test, the response of a reservoir to changing injection is monitored. A change in the flow rate usually results in changes in pressure which can be measured. Examples of parameters that control the reservoir response are storativity, transmissivity (permeability), wellbore storage, wellbore skin, fracture properties and reservoir boundaries. A mathematical model is commonly set up to simulate the transient pressure response in the well and the reservoir, due to an instantaneous step change in injection or production. The mathematical model depends on values selected for properties characterising the reservoir and by iterating these values such that

the modelled response fits the observed data one can infer the characteristic properties of the reservoir (Horne, 1995). The pressure diffusion equation is the basis of all models in well-testing theory or pressure transient analysis.

The pressure diffusion equation is used to calculate the pressure (p) in the reservoir at a certain distance (r) after a given time (t) and from an injection (or production) well receiving or producing fluid at a specific rate (Q), starting at time t = 0. The pressure diffusion equation is derived by combining the conservation of mass law, Darcy's law and the equation of state of the fluid.

The following assumptions are made before the derivation of the equation (Horne, 1995 and Haraldsdóttir, 2016):

- Horizontal radial flow
- Darcy's law applies
- Homogeneous and isotropic reservoir
- Isothermal conditions
- Uniform thickness of reservoir h
- Single-phase flow
- Small pressure gradients
- Small and constant compressibility ct
- Constant porosity φ
- Constant fluid viscosity μ
- Constant permeability k

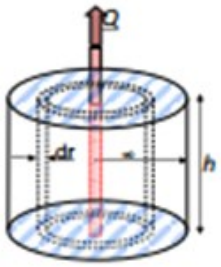

Figure 4: Radial flow through a cylindrical shell around a well (Haraldsdottir, 2016)

Law of conservation of mass: mass flow in – mass flow out = mass rate of change within the control volume. C consider the flow through a cylindrical shell of thickness, dr, situated at a distance, r, from the centre of the cylinder (Figure 4).

Then applying the law of conservation mass:

$$\left(\rho Q + \frac{\delta(\rho Q)}{\delta r} dr\right) - \rho Q = 2\pi r \frac{\delta(\varphi \rho h)}{\delta t} dr$$

$$or, \ \frac{\delta(\rho Q)}{\delta r} = 2\pi r \frac{\delta(\varphi \rho h)}{\delta t} \quad (1)$$

where, ρ, φ, Q, r, t, h represent Density (kg/m^3), Porosity (ratio 0<φ<1), Volumetric flow rate (m^3/s), Radial distance (m) from the well, Time (s) and Reservoir thickness (m), respectively.

Darcy's law or the law of conservation of momentum

Darcy's law in radial form is:

$$(Q = 2\pi rhk/\mu \ \ \delta p/\delta r) \quad (2)$$

where p, μ, k are Pressure (Pa), Dynamic viscosity (Pa. s) and Formation permeability (m^2), respectively.

Equation of state of the fluid (fluid compressibility at constant temperature) can be expressed as:

$$(Cw = \ 1/\rho \ \ \delta\rho/\delta p) \quad (3)$$

where Cw is Fluid compressibility.

By combining Equations 1, 2, and 3, we obtain the pressure diffusion equation given by:

$$\frac{1}{r}\frac{\partial}{\partial r}\left(\frac{r\,\partial p(r,t)}{\partial r}\right)=\frac{\mu c_t}{k}\frac{\partial p(r,t)}{\partial t}=\frac{S}{T}\frac{\partial p(r,t)}{\partial t} \quad (4)$$

$$\frac{\partial^2 p}{\partial r^2}+\frac{1}{r}\left(\frac{\partial p(r,t)}{\partial r}\right)=\frac{\mu c_t}{k}\frac{\partial p(r,t)}{\partial t}=\frac{S}{T}\frac{\partial p(r,t)}{\partial t}$$

Equation 4 is the basic equation for well testing. Solutions for this equation can be obtained for different regimes depending on the initial and boundary conditions, but that is beyond the scope of this project.

3.2 Injection well test process and analysis

An injection test is done by lowering a pressure tool to a selected depth near to a major permeable zone in the well. Water is pumped into the well at different pumping rates. In some cases, there is some fixed injection for a while before starting the test, allowing the pressure to stabilise, but in other cases, there is no injection until the step test starts, e.g. in the injection tests from Aluto Langano. The first pumping rate in the test is held at a constant rate to allow the pressure to stabilise. The pumping rate is then changed stepwise, and each step should be long enough to allow the pressure in the well to stabilize again. This process is repeated for several pumping rates. In some countries, the pump is turned off at the end of the well test, and the well is monitored and allowed to return to its natural pressure, which is the so called fall off test. Through all this process, the well pressure is recorded as a function of time.

The analysis of the injection test is done using the software Welltester version 2 (WT) (Marteinsson, in publication) to handle data manipulation and analysis of well tests (mainly multi-step injection tests) and presents the results both graphically and in tables. The software works like this: (Haraldsdóttir, 2016, Marteinsson, in publication).

- Initial parameters: The reservoir temperature, rock type and porosity are fed into the program, and the pressure is deduced by WT; these values are used to calculate approximate values of the dynamic viscosity of the reservoir fluid and the total compressibility of the rock matrix and the fluid; The wellbore radius which is the average radius of the well below the production casing the reservoir depth is also fed into the program.
- Set steps: The initiation time of injection steps is selected on the graph
- Modify: This step is designed to clean, correct and resample the data
- Model: In this step, the most appropriate model for the reservoir being investigated is selected. To achieve this, the derivative plot is used, along with the pressure data as a function of time on graphs with a log-log scale as well as linear and log-linear scale.

The main parameters deduced from the Welltester simulation are explained in the manuals of WellTester and Welltester V2 (Júliusson et al., 2008, Marteinsson, in publication) as follows:

Transmissivity describes the ability of the reservoir to transmit fluid, hence largely affecting the pressure gradient between the well and the reservoir. Its physical formulation is (kh/μ), where k is the effective permeability of the reservoir, h is the reservoir thickness, and μ is the dynamic viscosity of the active reservoir fluid. Level of stabilisation of the derivative plot is inversely proportional to μ/kh which means that if you have low stabilization of derivative plot, the result will be high kh and visa verse. Stabilisation of the derivative plot is indicative of the radial flow of fluid into the well.

Storativity defines the volume of fluid stored in the reservoir, per unit area, per unit increase in pressure [m3/(pa*m2) or m/Pa]. How fast the pressure can travel within the reservoir depends on the storativity of the reservoir. Storativity depends on fluid compressibility. It varies greatly between reservoir types, i.e. liquid dominated vs two-phase or dry steam. Common values for liquid dominated geothermal reservoirs are around 10-8 [m3/ (pa*m2) or m/Pa] and 10-5 [m3/(pa*m2) or m/Pa] for two-phase reservoirs.

Skin factor (S) is a variable used to quantify the permeability of the volume immediately surrounding the well. This volume is often affected by drilling operations, being either damaged (e.g. because of drill cuttings clogging the fractures) or stimulated (e.g. due to extensive fracturing around the well). For damaged wells, the skin factor is positive, and for stimulated wells, it is negative.

The injectivity index (II) is often used as a rough estimate of the connectivity of the well to the surrounding reservoir. Mathematically injectivity is defined as the change in the injection flow divided by the change in the stabilised reservoir pressure, and its unit is (L/s/bar).

Wellbore storage (C) is defined as the difference between the wellhead flow rate and the sand face flow rate (i.e. the flow into or out of the actual formation).

The radius of investigation (re) is the approximate distance at which the pressure response from the well becomes undetectable.

Statistical parameters, e.g. the Coefficient of variation (CV), is defined as the ratio between the standard deviation σ and the mean value μ for the particular parameter in the model. The lower the value of CV is the better the modelling.

3.3 Injection well tests in Aluto-Langano

Injection step tests from LA-3 and LA-10D were simulated, recordings were scarce from the test in LA-3 which was done in the 1980s but abundant from LA-10D which was done recently, technically much better. Yet it was possible to simulate both of them with WT with some extra data manipulation.

Table 2 and 3 show the selected initial parameters and the selected model for the Welltester analysis of the injection tests from both of the wells.

Table 2: Initial parameters used in the well test analysis of LA-3 and LA-10D where those marked with * are inserted by the user as well as the type of rock.

Name of Parameters and units	LA-3	LA-10D
Estimated reservoir temperature [°C] *	300	300
Estimated reservoir pressure [bar-g]	97	91.45
Wellbore radius, r, [m] *	0.11	0.11
Porosity, φ *	0.1	0.1
Dynamic viscosity of reservoir fluid, μ, [Pa.s]	8.962×10^{-5}	8.6×10^{-5}
Compressibility of reservoir fluid. c_w, [Pa^{-1}]	2.4413×10^{-9}	3.14×10^{-9}
Compressibility of rock matrix, c_r, [Pa^{-1}]	2.44×10^{-11}	2.44×10^{-11}
Total compressibility. C_t, [Pa^{-1}]	2.66×10^{-10}	3.36×10^{-10}

Table 3: Model selected for injection tests in wells LA-3 and LA-10D

Reservoir	Homogeneous
Boundary	Constant pressure
Well	Constant skin
Wellbore	Wellbore storage

3.3 LA-3

The third deep exploration well of the Aluto-Langano geothermal field, LA-3 was drilled between the 21 January and 13 June 1983. The well was completed at 2143.9m, and the maximum measured temperature was 309 °C at 1834m after 132 hrs of the warm-up period. Loss of circulation encountered up to 10.5 l/s below 1890m and complete loss of up to 29.2 l/s occurred between 2117m and 2143.9m (Bödvarsson, 1986). The injection test in LA-3, consisted of three injection steps (9.7, 19.7 and 28.2 l/s) with increasing injection rates, followed by a falloff period as step nr. 4. In Bödvarsson's report from 1986, Figure 8 shows the injection/falloff data in a graph for well LA-3 (ELC, 1986). More points were added to injection steps of Figure 4 by reading off the graph because it was not possible to simulate well with what was provided numerically for this project and this had been done previously.

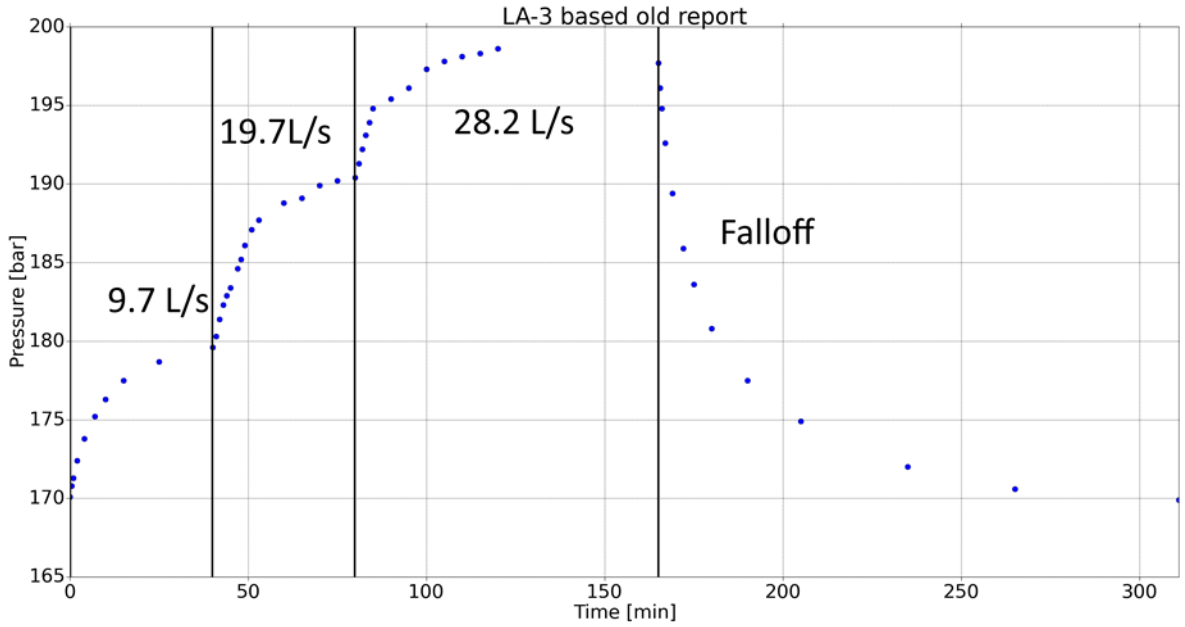

Figure 5: LA-3 pressure response and injection rate against time in four injection steps with a total duration of 5.2 hours.

Table 4: Reservoir parameters from nonlinear regression model for well LA-3

Parameter	Step 1	CV %	Step 2	CV %	Step 3	CV %	Step 4	CV %
Transmissivity, T ($m^3/(Pa.s)$)	2.7×10^{-9}	5.5	1.1×10^{-8}	35.2	2.8×10^{-9}	14.9	5.7×10^{-9}	0.4
Storativity, S ($m^3/(m^2Pa)$)	7.6×10^{-8}	3.4	1×10^{-8}	381.8	6×10^{-8}	12.8	5.5×10^{-8}	1.2
Radius of investigation, r_e (m)	10	3	10	319.3	17	13.6	104	2.7
Skin factor, s	-2.9	-	3	-	-3.2	-	-2.3	-
Wellbore storage, C (m^3/Pa)	3.1×10^{-6}	1.7	5.7×10^{-6}	1.9	2.5×10^{-6}	11.4	4.8×10^{-6}	0.5
Reservoir thickness, h (m)	284		23		227		206	
Permeability, k (m^2)	9×10^{-16}		4.3×10^{-14}		1.1×10^{-15}		2.5×10^{-15}	
Injectivity index, II ((L/s)/bar)	1.1		1.0		1		1	
Porosity, φ	0.1		0.1		0.1		0.1	

The reservoir parameters for all steps are shown in Table 4, and step four (the fall off step) was selected as the best model, having lower CV values (Júlíusson et al., 2008) than the other steps. Clearly, the modelling of step nr. 2 does not show good results with high CV in general. There the skin factor is positive but negative between -2.3 and -3.2 in the other steps, so the closest surroundings of the well have higher permeability than the reservoir, having the effect that well acts as if its radius is larger than the real radius. The transmissivity is rather low, and the storativity is relatively good. Figure 5 shows the results of the analysis of pressure against time in a logarithmic scale (A) and log-log scale (B). The log-log scale graph of pressure and time shows the derivative of pressure response multiplied by the time passed since the beginning of the steps. Derivative plots help determine the best reservoir model. As we can see from Figure 5, the model fits the collected data fairly well.

Modelling of Step-4

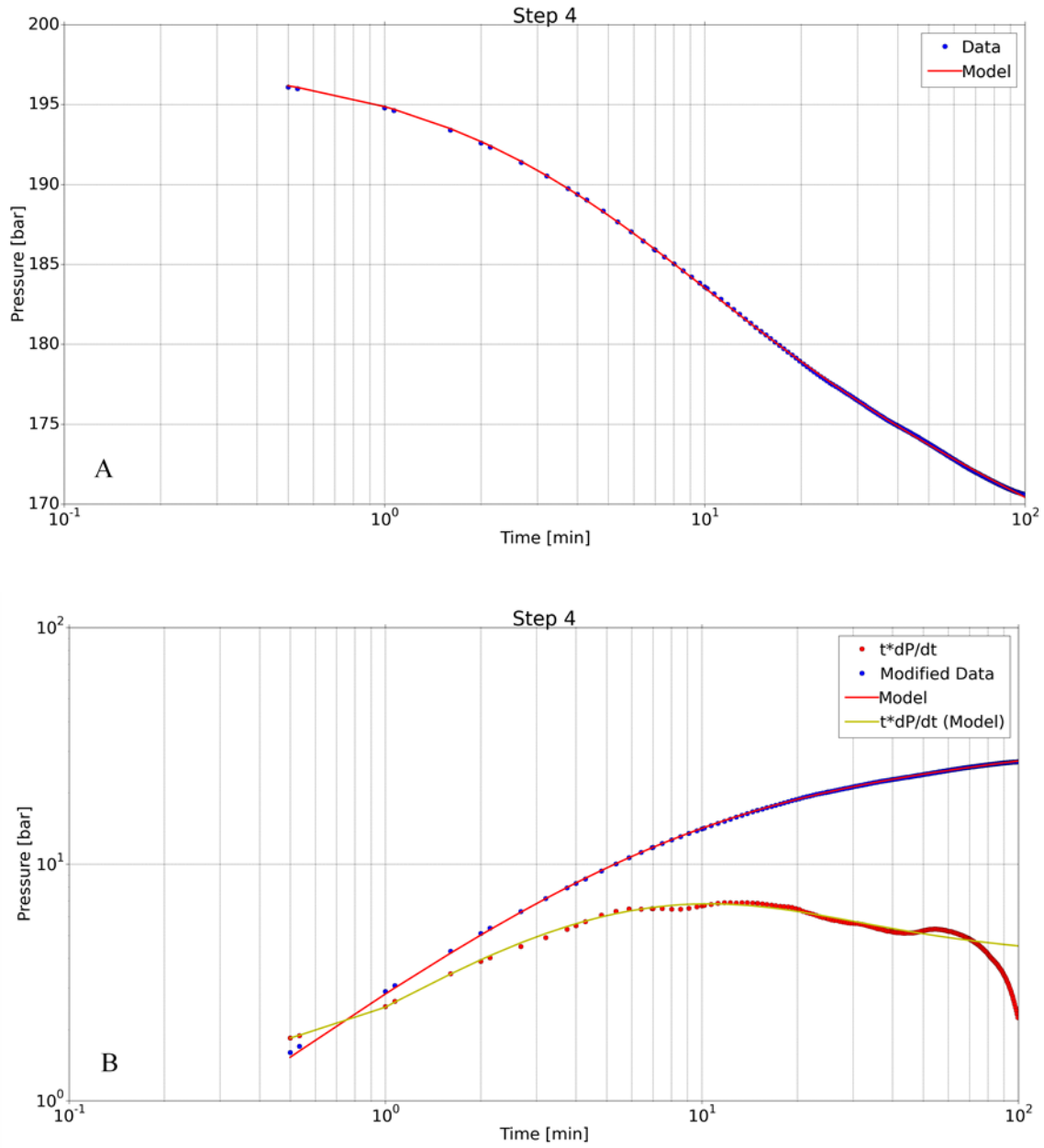

Figure 6: LA-3, model results and recorded pressure for step 4 using a logarithmic time scale (A) and log-log scale including the derivative (B)

3.4.2 LA-10D

This is the second directional well drilled in Aluto-Langano geothermal project. It is the 10th deep well completed in October 2015. The well is drilled to the maximum measured depth of 1940m in the direction of N43°W with an inclination of 28° and with a maximum measured temperature of 310°C at the bottom of well. The directional drilling kick off point (KOP) is 450m. The pressure-temperature spinner (PTS) tool was set at 551m depth, and the water injection at the rate increased from 0 l/s to 14.9 L/s. After that, the injection rate was increased to 17, 19.3 and 21.7 L/s in the following steps and the pressure in the well was recorded. The injection rate of each step was one hour.

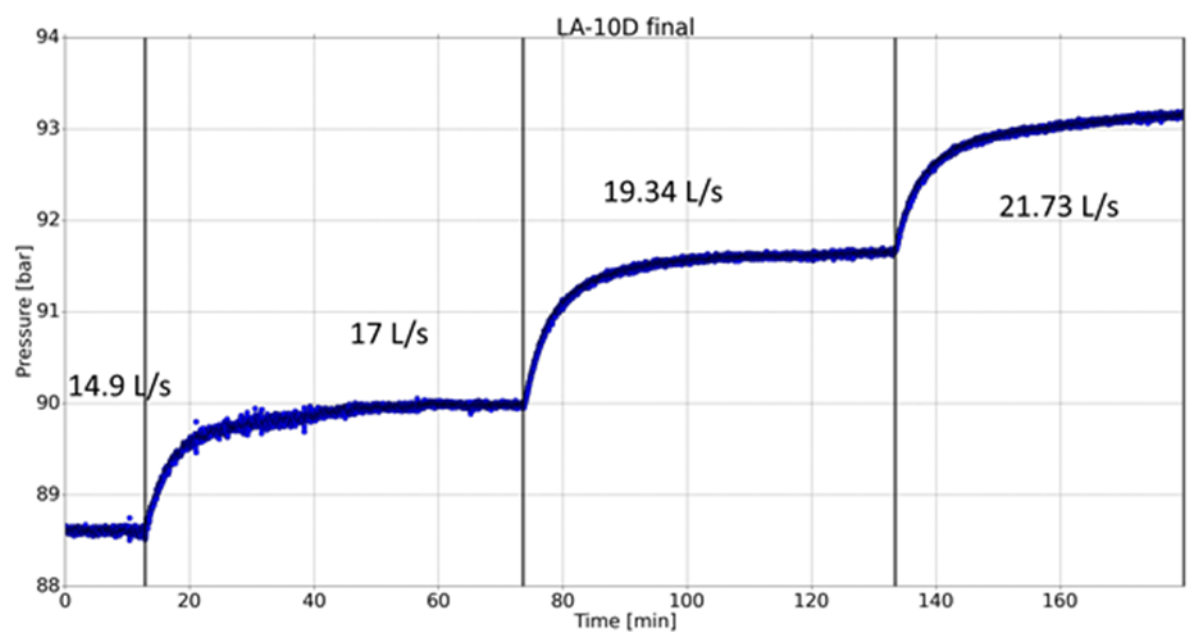

Figure 7: LA-10D pressure response and injection rate against time in three injection steps with a total duration of 3 hours

The resulting reservoir parameters from the model for all steps are shown in Table 5, and the results for step three were selected as the best ones, having lower CV values than the other steps (Júlíusson et al., 2008). The results show relatively good transmissivity and storativity, but the skin factor is not so good.

Table 5: Reservoir parameters from nonlinear regression model for well LA-10D

Parameter	Step 1	CV %	Step 2	CV %	Step 3	CV%
Transmissivity, T (m^3/(Pa.s))	1.3×10^{-8}	0.7	2×10^{-8}	0.7	1.3×10^{-8}	0.4
Storativity, S ($m^3/(m^2Pa)$)	5.1×10^{-8}	2.2	3×10^{-8}	3.4	5.7×10^{-8}	2.1
Radius of investigation, r_e (m)	122	5.6	62	2.4	119	4.8
Skin factor, s	0.07	-	3.1	-	-0.3	-
Wellbore storage, C (m^3/Pa)	3.1×10^{-6}	0.68	4.1×10^{-6}	0.24	4.3×10^{-6}	0.3
Reservoir thickness, h (m)	152		87		168	
Permeability, k (m^2)	7.1×10^{-15}		1.9×10^{-14}		6.8×10^{-15}	
Injectivity index, II ((L/s)/bar)	1.4		1.4		1.6	
Porosity, φ	0.1		0.1		0.1	

Figure 8 shows the result of the analysis of pressure against time in a logarithmic scale (A) and log-log scale (B). The log-log scale graph of pressure and time shows the derivative of pressure response multiplied by the time passed since the beginning of the steps. Derivative plots help determine the best reservoir model. As we can see from Figure 8, the model fits fairly well the collected data.

Modelling of Step-3

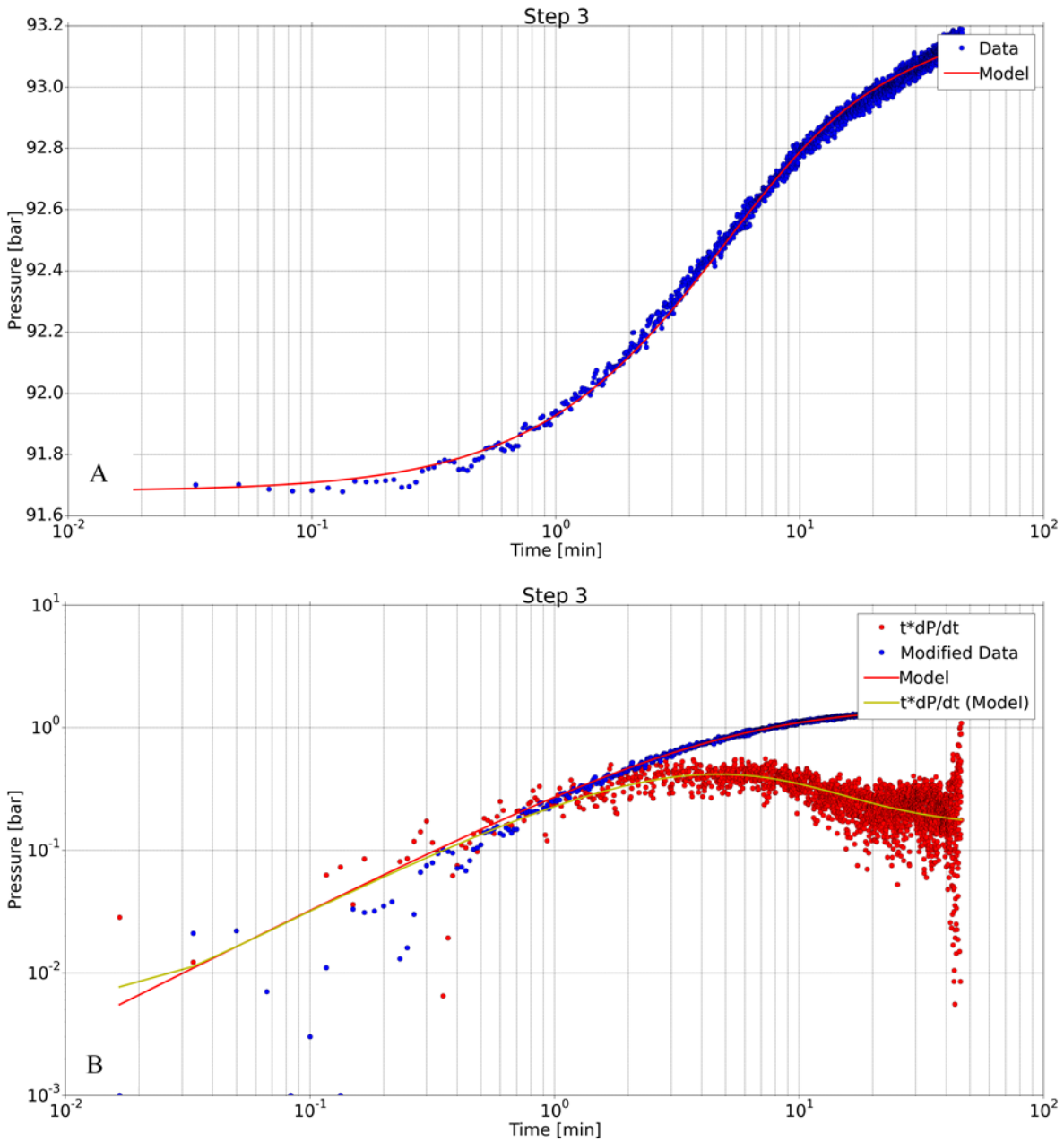

Figure 8: LA-10D, model results and recorded pressure for step 3 using a logarithmic time scale (A) and log-log scale including the derivative (B)

Injection well test analyses were done for wells LA-3, and LA-10D gave the best result for step number 4 and 3 respectively (Table 6) using a model assuming homogenous reservoir and constant boundary pressure. The skin factor values for the selected model steps are negative in both wells, which indicates that the nearest surroundings of the wells have higher permeability than the surrounding reservoir. The results (Tables 4 and 5)) show in general better transmissivity in LA-10D than in well LA-3 and relatively good storativity as in LA-3. The skin factor, on the other hand, is not particularly good in LA-10D and not as good as in well LA-3.

The injectivity indices are rather low in both of the wells, but higher in the new well, LA-10D, than in LA-3. Both wells LA-3 and LA-10D are characterised to be in liquid dominated reservoir.

Table 6: Estimated reservoir parameters of LA-3 and LA-10D from the best model and best step

Parameter	LA-3		LA-10D	
	Step 4	CV %	Step 3	CV %
Transmissivity, T (m^3/(Pa.s))	5.7×10^{-9}	0.4	1.3×10^{-8}	0.4
Storativity, S ($m^3/(m^2Pa)$)	5.5×10^{-8}	1.2	5.7×10^{-8}	2.1
Radius of investigation, r_e (m)	104	2.7	119	4.8
Skin factor, s	-2.3	-	-0.3	-
Wellbore storage, C (m^3/Pa)	4.8×10^{-6}	0.4	4.1×10^{-6}	0.3
Reservoir thickness, h (m)	206		168	
Permeability, k (m^2)	2.5×10^{-15}		6.8×10^{-15}	
Injectivity index, II ((L/s)/bar)	1.0		1.6	
Porosity, φ	0.1		0.1	

4 ANALYSIS OF FORMATION TEMPERATURE AND INITIAL PRESSURE PROFILES

4.1 Introduction

Temperature and pressure logs are used extensively in geothermal exploration and development. The temperature and pressure logs are carried out during drilling of wells, during heating up, after drilling and during flow tests as well as for monitoring. During drilling, the well temperatures are highly disturbed by drilling fluid circulations, with cold water injected into the well. During drilling, the temperature logs provide valuable information on the location of aquifers (feed zones) and their relative sizes (permeability). Internal flow often exists in very permeable wells with multiple feed zones. This flow is seen in temperature logs as the constant temperature in the depth interval between feed points in the well, and sometimes the internal flow rate can be estimated based on temperature transients (Steingrimsson, 2013).

In the geothermal investigation, temperature and pressure logging is important in determining formation temperature and reservoir pressures. The temperature and pressure disturbances in a well during drilling will fade away gradually after the drilling stops. The wells will heat up and reach thermal equilibrium with the surroundings in a matter of several months, and the well pressures will also recover after drilling and reach equilibrium with the permeable feed zones of the well. Temperature and pressure logs during the recovery period after drilling are the most important data to estimate formation temperatures and reservoir pressure (Steingrimsson, 2013).

Conditions inside the well during logging are not the same as in the surrounding formation or as undisturbed conditions in the reservoir before drilling. Different methods are used to estimate the formation temperature and pressure. Formation temperature can be estimated by extrapolation of a short term temperature data from the well logs during the warm-up at selected depth for each estimation using the Horner plot method (Steingrimsson, 2013).

The Horner plot method

The Horner plot method is a simple analytical technique used for analysing temperatures to determine the formation temperature (Helgason, 1993). The basic criterion for the technique is the straight-line relationship between measurements of temperatures at the selected depth and ln(τ),

$$\tau = \frac{\Delta t}{\Delta t + t_0} \quad (5)$$

where τ, Δt, t_0 are Horner time, the time passed since circulation stopped and the circulation time respectively.

By using the above equation, one can plot the wellbore temperature at the selected depth from logs during the warm-up as a function of ln(τ) and then plot a straight line through the data by which the extrapolation to ln(τ) = 0 we estimate the formation temperature (Helgason, 1993).

A computer software from the ICEBOX package, Berghiti, is used for estimation of formation temperatures (Arason et al., 2004; Marteinsson, personal communication in August 2016).

The reservoir pressure is estimated from data obtained during the recovery period. It is determined with the help of another software called Predyp from ICEBOX (Arason et al., 2004) by feeding the obtained formation temperature as a function of vertical depth and known initial wellhead pressure or water level. The warm-up pressure profiles are plotted to determine their intersection, known as pivot point which shows the depth and pressure at the best zone in the borehole and can be considered as the actual pressure value in the reservoir.

In sections 4.2 and 4.3, the temperature and pressure profiles are analysed to determine the formation temperatures and estimate the initial reservoir pressure for Aluto-Langano wells LA-9D and LA-10D. The temperature and pressure measurements in these wells were performed during injection and warm-up of the wells, but only logs during warm-up can be utilised to find the formation temperature. Figure 9 shows an example of results from BERGHITI.

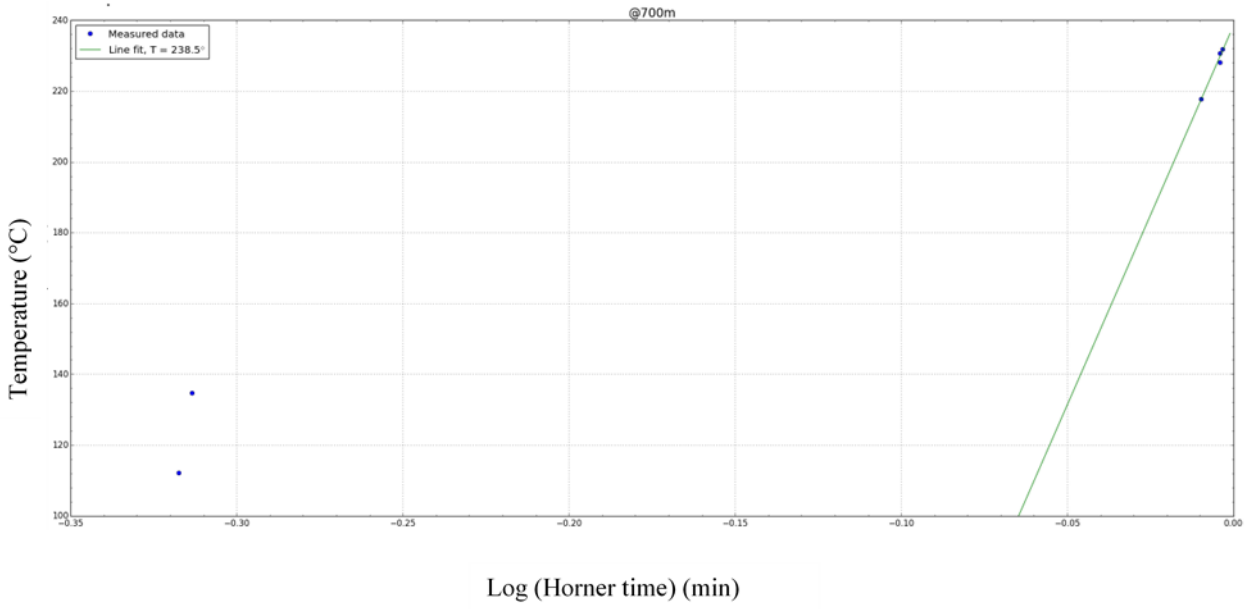

Figure 9: Formation temperature at 700 m in well LA-9D estimated with Horner method

4.2 Well LA-9D

Drilling of well LA-9D was started on November 12, 2013. Drilling of this well was interrupted due to repeated loss of circulation and insufficient water supply system to continue drilling blind. After procurement of water supply pumps and equipment, drilling was re-started in February 1, 2015, and was completed on April 30, 2015. The directional drilling kick-off (KOP) is at 700m to a direction of N70°W with 51° maximum inclinations.

TABLE 7: Depths and casing depths in LA-9D with respect to ground surface and information about casings

Depth (m)	Vertical depth(m)	Bit size (")	Casing diameter (")	Casing depth (m) from the ground surface
60	60	26	20	56.7
210	210	17 ½	13⅜	207.9
608	608	12 ¼	9⅝	605
1920	1785	8 ½	7	1915

In well LA-9D seven small feed zones were located at 760 m, 830 m, 940 m, 1000 m, 1136 m, 1585 m and 1707 m vertical depth, while a large feed zone was encountered at 1333 m vertical depth. The feed zones were identified from logs during injection and warm-up logs and with the help of loss of circulation data sets.

The water injection to the well was stopped at 00:00 on 7 May 2015, and the temperature recovery was monitored. The logging during the warm-up period was done with a PTS (pressure, temperature, spinner) tool on 7, 8 and 9 May. Additional measurement was carried out on 1 June to check the well temperature condition, and PTS was carried out on 5 May. However, due to problems at the spinner part of the tool, only pressure and temperature were obtained (WJEC, 2015).

The temperature recovered steadily, and the temperature below 1870 m depth exceeded 250°C during the log on May 7. The logging survey on May 9 recorded more than 280°C around the well bottom of about 1900 m depth. The temperature on June 1 had recovered slightly more than during the first warm-up logs. Focusing on the production zone of the well, the measured temperature is 192°C, at casing shoe (605 m) and 306°C, at the maximum logging depth (1911 m) in the log from 1 June (Figure 10).

The formation temperature was estimated from the data set obtained during the temperature recovery of the well. The estimated formation temperature increases with depth and reaches about 309°C at the well bottom.

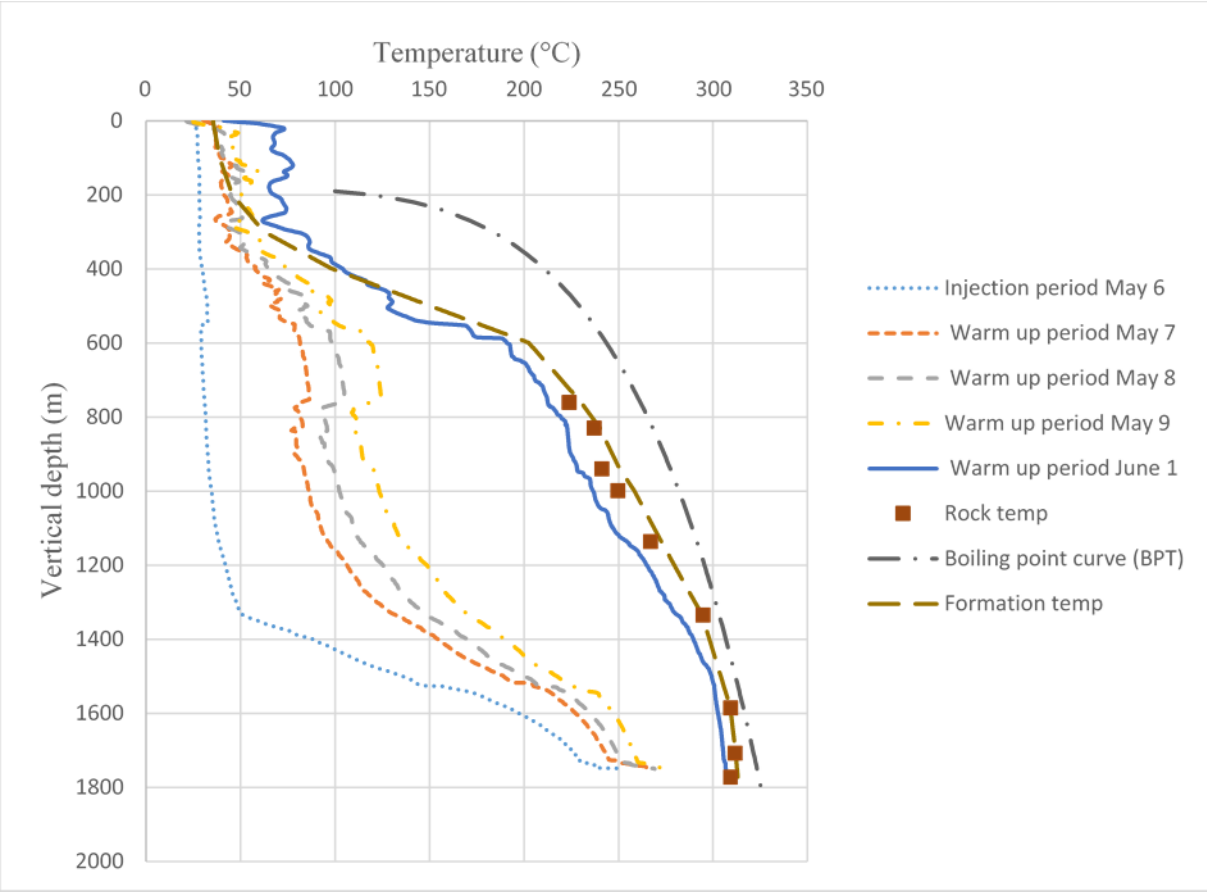

Figure 10: Temperature logs with injection, during warm-up, boiling point curve (BTP) and estimated formation temperature of LA-9D

The data points to be used in the BERGHITI programme were selected from the temperature logs at a depth of the feed zones, and their estimated formation temperature was determined and then plotted in Figure 9 with the temperature logs with vertical depth. The formation temperature of the well was estimated from these points. The formation temperature increases in the production part of the well to 300-311°C.

To calculate the initial pressure, the estimated formation temperature profile from Figure 10 was used as input to the PREDYP program. The water level was adjusted in the calculations until the calculated profile matched the pivot point pressure. The pressure match was achieved with water levels at approximately 200 m vertical depth.

The pressure profile obtained during the warm-up period and the initial pressure profile are shown in Figure 11 against vertical depth. The pivot point of LA-9D is located at 1100 m vertical depth with the pressure of 85 bar.

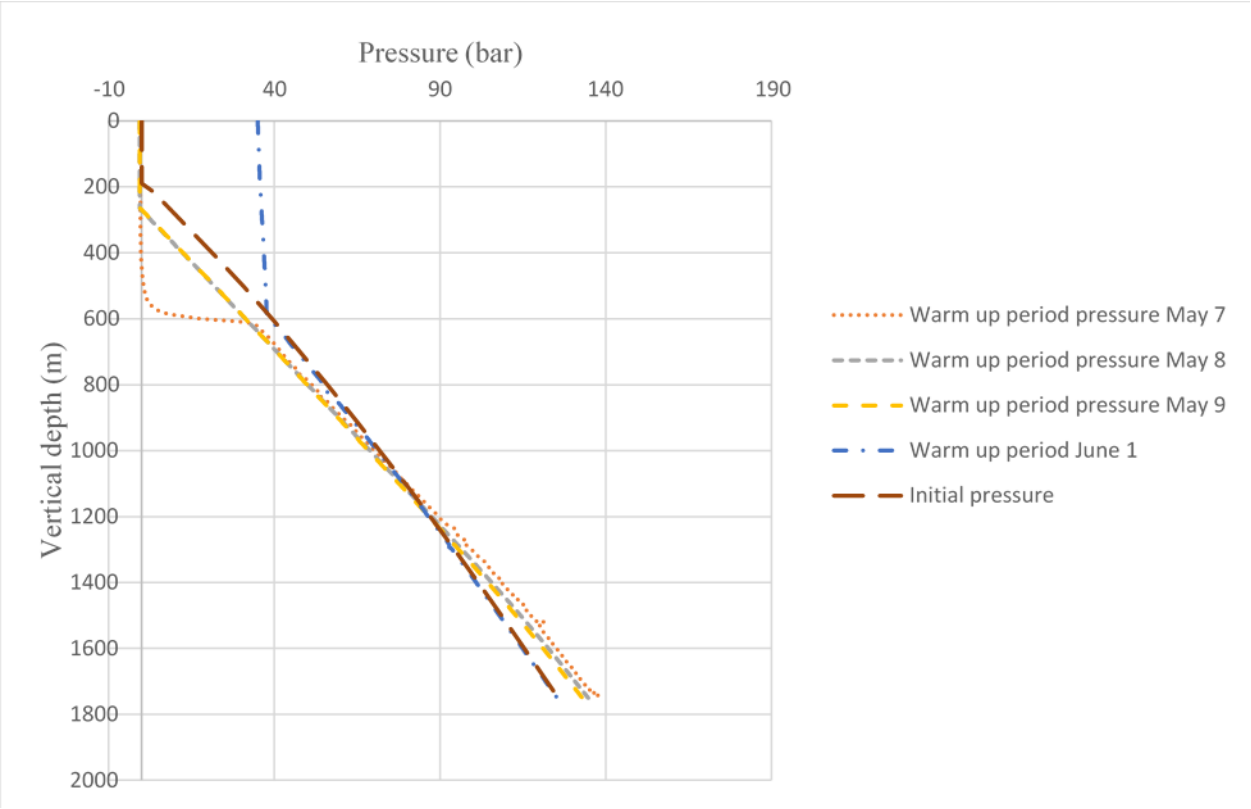

Figure 11: Pressure logs during the warm-up period and estimated initial pressure of LA-9D

4.3 Well LA-10D

Drilling of well LA-10D was started on June 25, 2015, and completed on October 2, 2015. The directional drilling kick off point (KOP) is at 450m to a direction of N43°W with a maximum inclination of 28°.

TABLE 8: Depths and casing depths in LA-10D with respect to ground surface and information about casings

Depth (m)	Vertical Depth (m)	Bit size (")	Casing diameter (")	Casing depth (m) from the ground surface
60	60	26	20	57.11
347	347	17 ½	13⅜	345
809	809	12 ¼	9⅝	807
1951	-	8 ½	7	1951
1825	1699	-	-	-

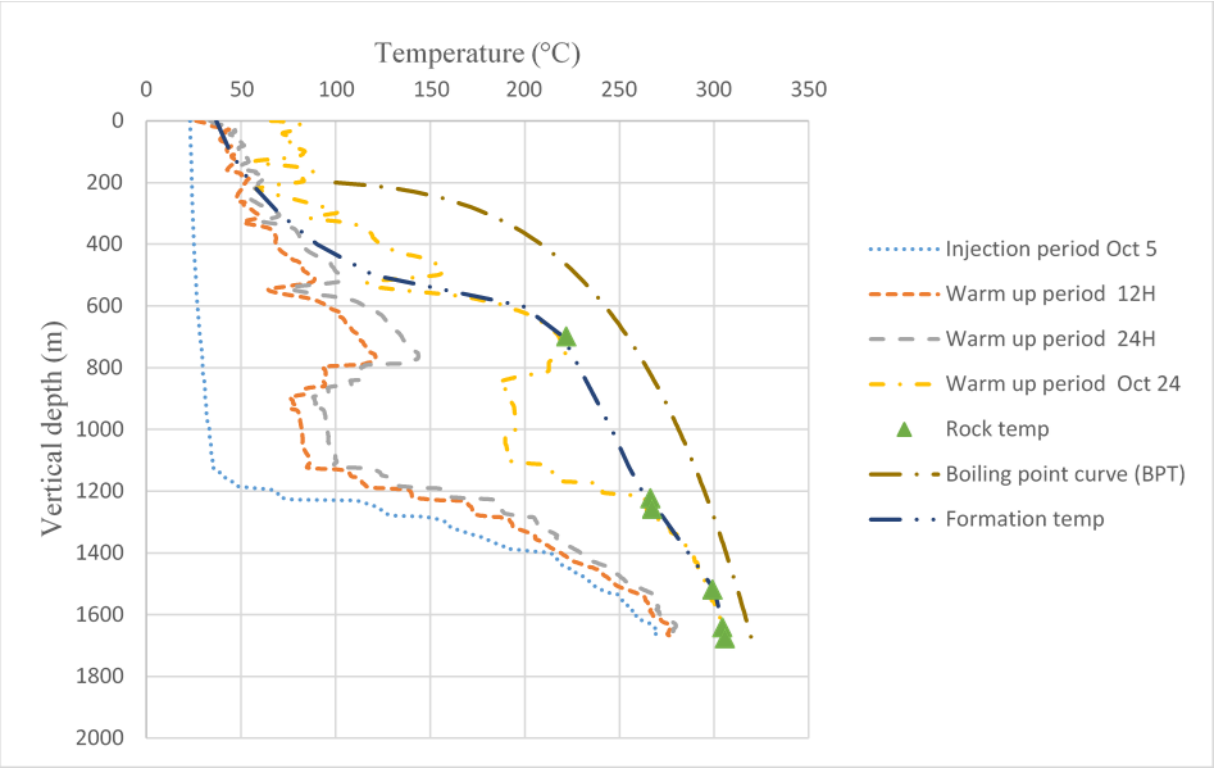

Figure 12: Temperature logs with injection, during warm-up, boiling point curve (BPT) and estimated formation temperature of LA-10D

In well LA-10D six small feed zones had been located at 909 m, 1244 m, 1260 m, 1519 m and1642 m, vertical depth, while large feed zone at 699 m vertical depth had been encountered (circulation loss zone).

The water injection to the well was stopped at 00:00 on 5 October 2015, and the temperature recovery was monitored. The monitoring logs were carried out after 12 hours, 24 hours, on October 6 and on October 24, 2015. Additional measurement was carried out on November 18 and November 19, 2015, to check the well temperature condition but not used in this study since the data recovered were of very poor quality.

The temperature recovered steadily, and the temperature below 1700 m depth exceeded 250°C in the first log after 6 hours warm-up. The logging survey on 24 October, the temperature of more than 300°C were recorded around the well bottom at about 1800 m depth. Focusing on the production zone of the well, the measured temperature is more than 200°C, at casing shoe (807 m) and more than 300°C at maximum logging depth (1800 m) depth (Figure 12).

The formation temperature was estimated from the temperature well logs during warm-up on 6 and 24 October (12 hours and 24 hours) respectively. Frequent temperature logging during warm-up is strongly advised since too few temperature logs from that period increase the uncertainty of the estimated formation temperature. The estimated formation temperature increases with depth and reaches about 305°C at the well bottom 1800m depth (Figure 12).

The data points to be used in the Berghiti programme were selected from the temperature logs at a depth of selected feed zones, their estimated formation temperature was determined and plotted with the well logs in Figure 12 against vertical depth.

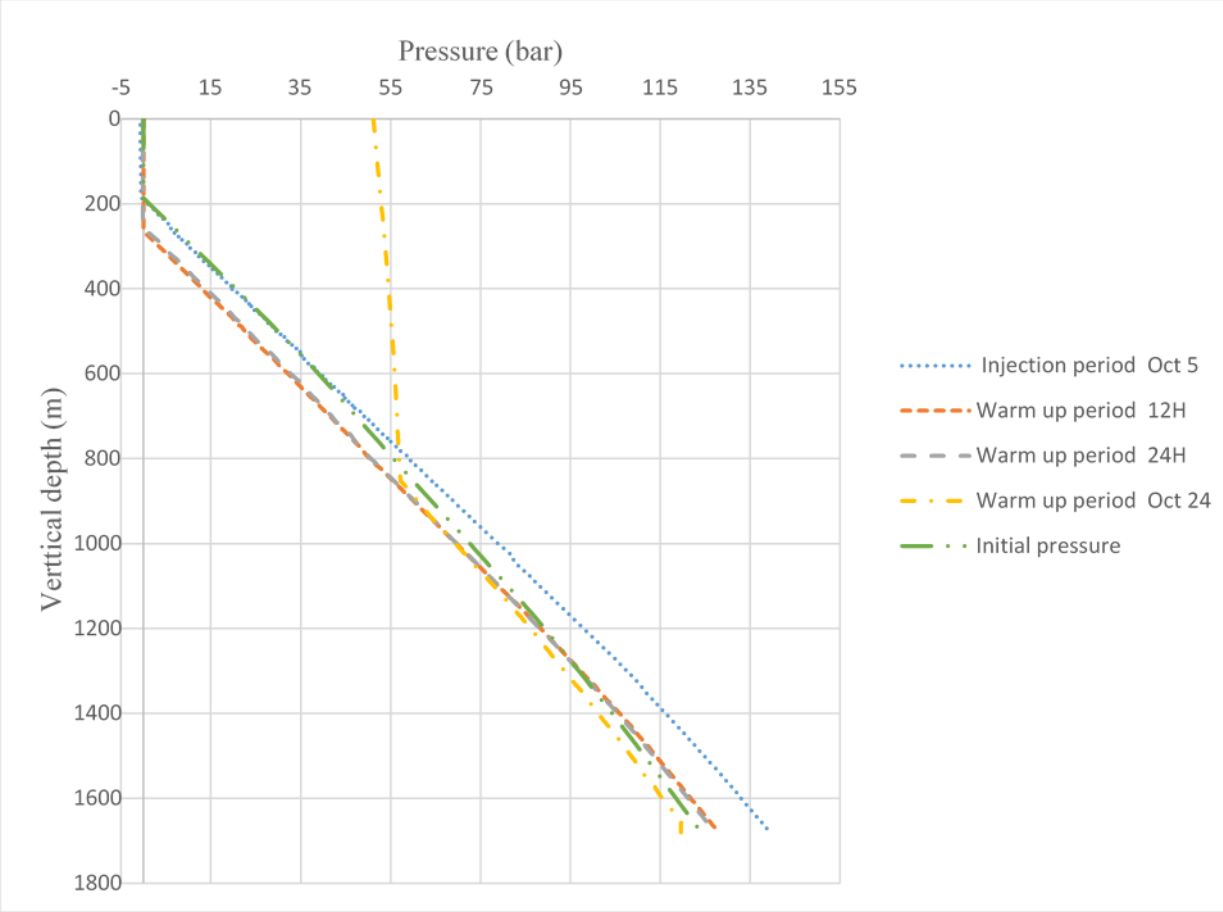

Figure 13: Pressure logs during the warm-up period and estimated initial pressure of LA-10D

To calculate the initial pressure, the estimated formation temperature profile from Figure 12 was used as input to the PREDYP program. The water level was adjusted in the calculations until the calculated profile matched the pivot point pressure. The pressure match was achieved with water levels at approximately 200 m depth.

The pressure profile obtained during the warm-up period and the initial pressure profile are shown in Figure 13 against vertical depth. The pivot point of LA-10D is located at 1200 m vertical depth with the pressure of 92 bar.

5. DISCHARGE TESTING

5.1 Introduction

Discharge testing is performed after a well has been allowed to warm up and recover its temperature. As the temperature of fluid increases during the warm-up period, in a high-temperature geothermal field wellhead pressure builds up in some of the wells. The first step in flow testing is starting the well discharge. For most wells, this is not difficult, since they naturally develop sufficient pressure, either cold gas or steam, so that opening the control valve will initiate flow. But in some wells, it can be difficult to start the flow. Even after waiting for weeks for the well to heat up, no pressure develops at the wellhead, and when the valve is opened there is no flow, this is most common in wellbores that have a cold section in the upper part of the well (Grant and Bixley, 2011). Different methods like gas lift, steam injection and workovers are used to stimulate geothermal wells.

During the warm-up period, the water level in the well will gradually rise and eventually build a wellhead pressure above atmospheric if the well is artesian. When the wellhead pressure has built up sufficiently, a discharge test can be conducted by flowing the well through an orifice (Bödvarsson and Witherspoon, 1989). Measurements can be performed to evaluate the total flow rate and enthalpy of the fluid. The lip pressure method (James, 1970) can be used to determine the total flow rate and enthalpy with a simple weir being used to measure liquid flow. By repeating these flow tests with different sized orifices, the well productivity as a function of wellhead pressure can be determined. That is one of the so-called characteristic curves for the well that can be used in selecting operating conditions for the turbines in the power plant (Bödvarsson and Witherspoon, 1989).

If environmental conditions permit, a short-term discharge test can be used with the lip pressure method to get a first estimate of the longer-term production potential and to determine the most suitable equipment for longer-term testing. The discharge can also help to clear debris from the well (Grant and Bixely, 2011). James lip-pressure method is used to determine the flow characteristics and production capacity of both wells LA-9D and LA-10D during discharge testing.

The lip pressure method is a convenient means of measuring the flow of many geothermal wells. It is based on an empirical equation developed by Russell James (1970) and is considered to be the most versatile method for testing all medium enthalpy wells.

Grant and Bixely, (2011); ‘‘To use this method, the steam-water mixture is discharged through an appropriately sized pipe into a silencer or some other device to separate the steam and water phases at atmospheric pressure (Figure 14). The lip pressure is measured at the extreme end of the discharge pipe using a liquid-filled gauge to damp out pressure fluctuations. Water flows from the silencer is measured using a sharp-edged weir near the silencer outlet.’’

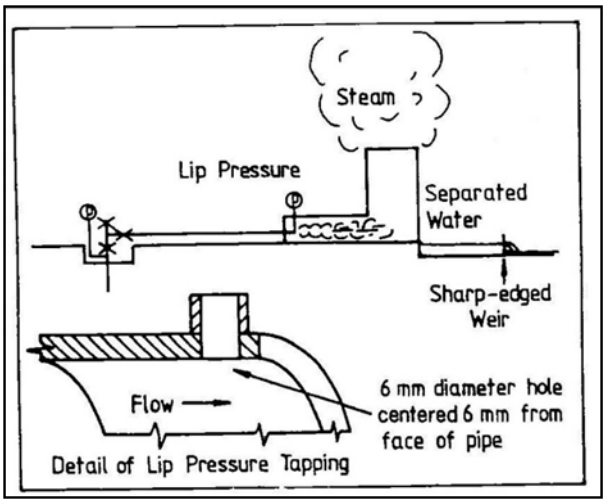

Figure 14: Flow measurement by lip pressure and silencer (Aris T. W et al., 2015)

Grant and Bixely, (2011) ‘‘James’s formula, relates mass flow, discharge pipe area, enthalpy, and lip pressure:

$$Q = \frac{183 p_{lip}^{0.96} A}{H_t^{1.102}} \tag{6}$$

where Q is the total flow rate in kg/s, P_{lip} is the lip pressure in bar-a, A is the cross-sectional area of the discharge pipe in cm^2 and H_t is the total enthalpy in kJ/kg.

When the flow is measured in tonnes per hour, equation 7 is used.

$$Q = \frac{663 p_{lip}^{0.96} A}{H_t^{1.102}} \tag{7}$$

The total mass flow rate obtained from James lip pressure measurement can be related to water flow rate measured at the silencer after flashing;

$$Q = \frac{H_s - H_w}{H_s - H_t} Q_w \tag{8}$$

where Q_w is the water flow rate measured at the silencer after flashing in kg/s, H_s and H_w are the saturated steam and saturated water enthalpies at the pressure of silencer measurement in kJ/kg

If we combine equations 1 and 3, we obtain;

$$\frac{Q_w}{AP^{0.96}} = \frac{184}{H^{1.102}} \frac{H_s - H_t}{H_s - H_\omega} \tag{9}$$

The steam mass fraction, X can be calculated as:

$$X = \frac{H_t - H_w}{H_s - H_w} \quad (10)$$

By measuring the lip pressure, water flow, cross-sectional area of the pipe, then the total enthalpy can be obtained numerically. The enthalpies of steam and water can be obtained with the help of steam table from their corresponding temperatures and pressures.''

With the help of the LIP program from the ICEBOX software package (Arason et al., 2004, Marteinsson, 2016), the enthalpies and flow rates are calculated considering weir properties correspond to a standard 90^0 V-notch weir box.

5.3 Discharge Testing of Well LA-9A

Figure 15 shows recordings during two flow tests in well LA-9D. The one-month long discharge test of well LA-9D was started on 4 November 2015 by opening the master valve, and the discharged geothermal fluid was sent to an atmospheric silencer. The mass flow data was measured every hour during the testing period. The different size of discharge pipe with a diameter of 3", 4", 5" and 6" was used to obtain the stable discharge mass flow data at different wellhead pressure. The lip pressure monitored as well as the wellhead pressure (WHP) and the height of the liquid in the weir-box. Fluid sampling was also carried out for chemical analysis. The well was closed on 4 December 2015 to finish the one-month single well discharge test.

The well LA-9D was discharged again on 10 January 2016 (Table 9) when well LA-10D was discharging continuously. The two wells were discharged simultaneously until the well LA-10D was closed on 1 June 2016. The PTS logging (flowing survey) was carried out on 18 March 2016 to obtain the data on flow conditions in the wellbore. The master valve of LA-9D was closed gradually from 27 May and completely shut off on 1 June 2016.

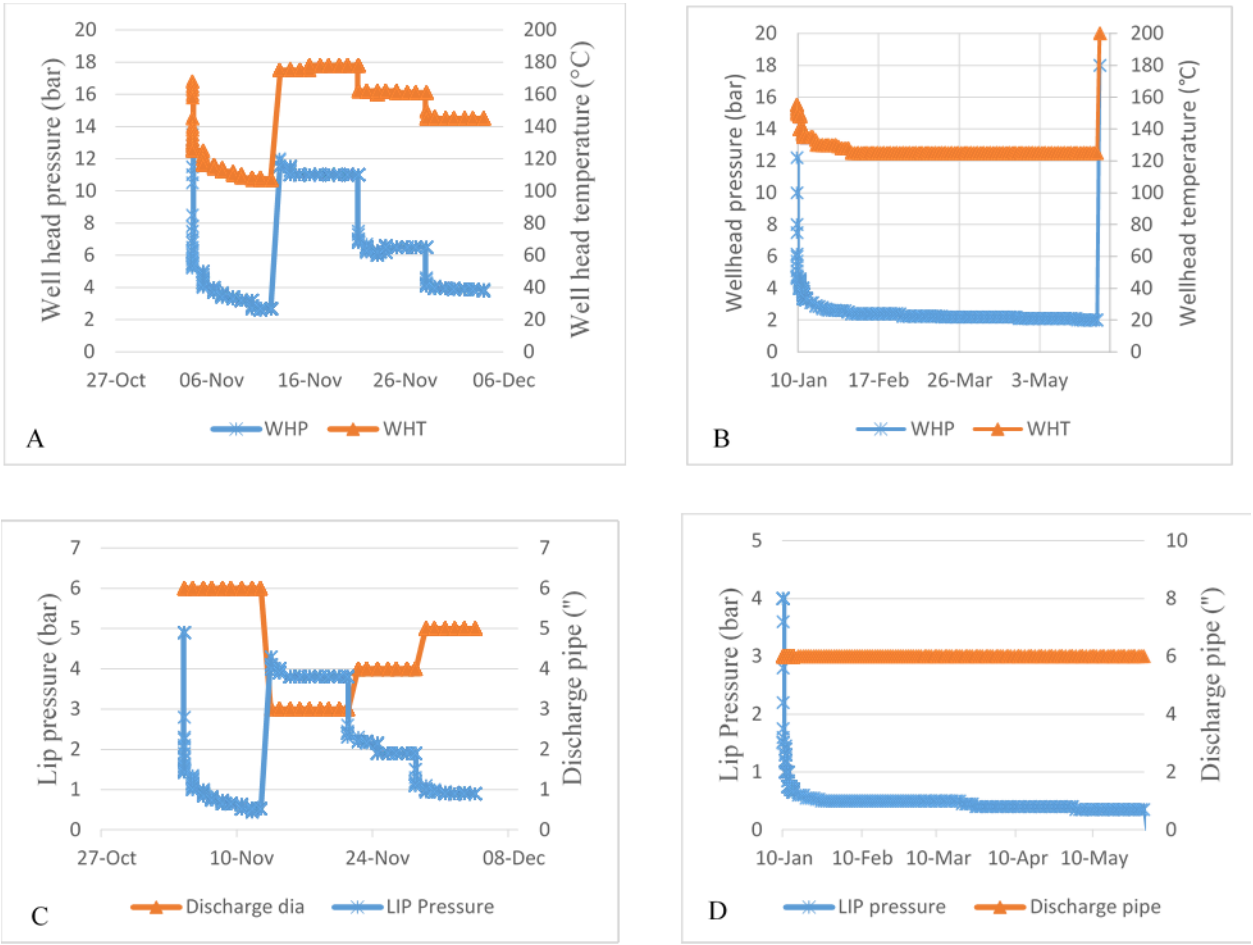

Figure 15: First (A and C) and Second (B and D) discharge test data of LA-9D well, showing wellhead pressure and temperature (A and B) and lip pressure and discharge pipe diameter (B and D)

The PTS logging at LA-9D was carried out on 18 March 2016. The fluid was discharged through 6" discharge pipe and the wellhead pressure and the total mass flow rate was 2.25 bar-g and about 10.61 kg/s, respectively.

Figure 15 shows wellhead temperature and wellhead pressure (A and B) and lip pressure and discharge pipe (C and D) of the first and second discharge.

The calculated water, steam, total mass flow rate and fluid enthalpy of the first and second discharge test of LA-9D are shown in Fig 16. At the beginning of the test and at the time of discharge pipe replacement, the flow rate is relatively higher but stabilises with time, even stabilized flow rate data where obtained with different discharge pipe size.

The analysis of the measurements from the single well discharge (first discharge) test of well LA-9D gives an estimate of steam flow in range of 4.7 – 11.2 kg/s at the separation pressure of 1 bar-a (Table 9) which is equivalent to 2.4 – 5.6 MW of electric power output assuming 2 kg/s of steam flow convert to 1 MWe. The steam flow rate at the wellhead of 6.5 bar-g was 6.49 kg/s, which is equivalent to 3.2 MWe.

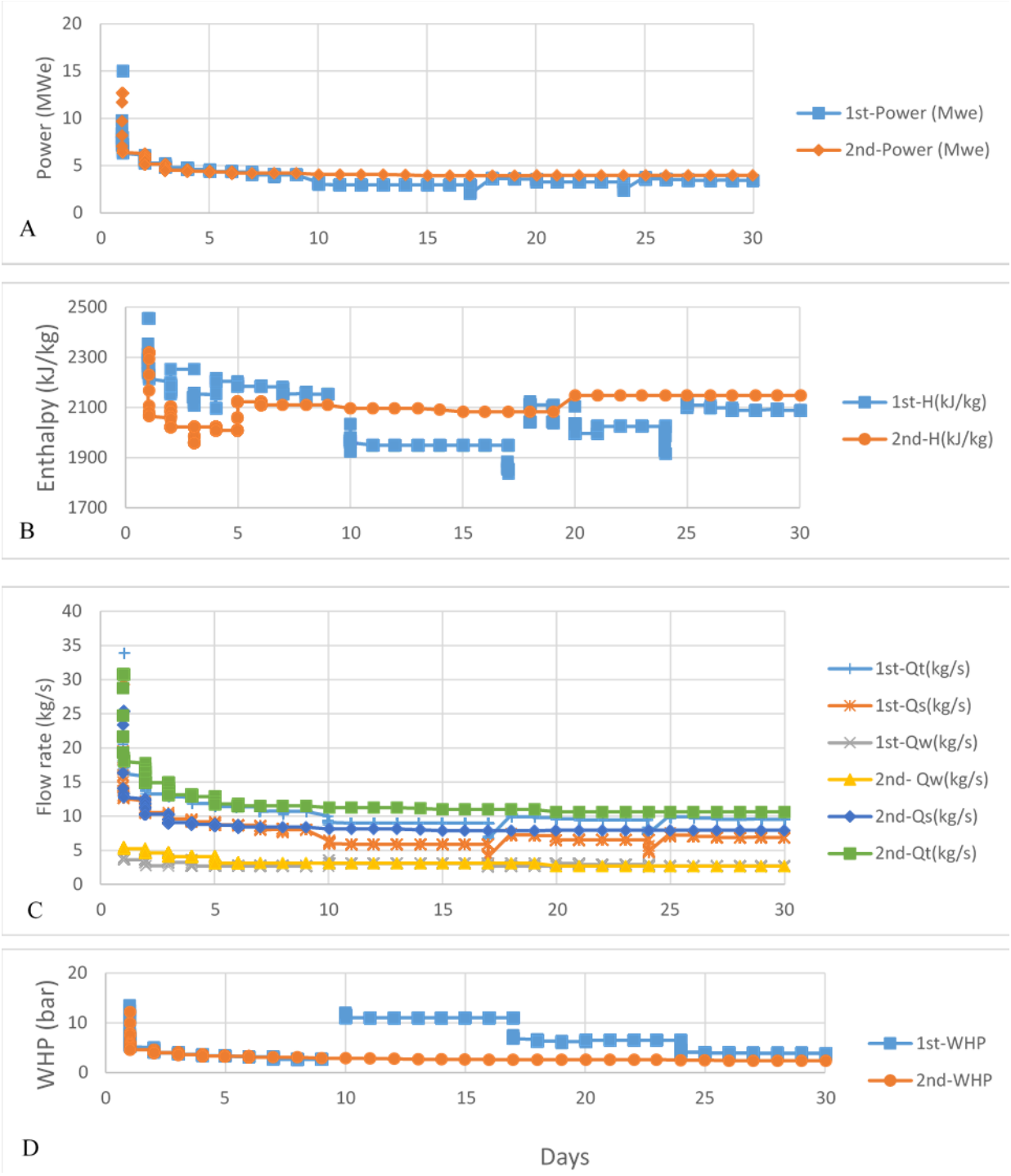

Figure 16: Results of first 30 days of LA-9D long term discharge test, after which it was constant (see Fig 15 B and D), showing wellhead pressure (D), flow rate (C), enthalpy (B) and power (A), in two flow tests (1st and 2nd)

Table 9: Measurements and results for well LA-9D from the Russel James lip pressure method with separation pressure of 1 bar-a

No	Date	P_0(bar)	P_c(bar)	D_p(inch)	W_{height}(cm)	H(kJ/kg)	Q_t(kg/s)	Q_w(kg/s)	Q_s(kg/s)	X
1	2015-11-12	2.7	0.5	6	8	2152.8	10.7	2.7	8	0.7
2	2015-11-20	11	3.8	3	8.5	1949.3	9	3.1	5.9	0.7
3	2015-11-27	6.5	1.9	4	8.3	2025.1	9.4	2.9	6.5	0.7
4	2015-12-04	3.8	0.9	5	8	2087.3	9.5	2.7	6.8	0.7
5	2016-05-27	2.3	0.5	6	8	2147.6	10.6	2.7	7.9	0.7

Table 10: Measurements and results for well LA-9D from Russel James lip pressure method with separation pressure of 5 bar-a as in the Aluto-Langano pilot power plant

Dp (in)	Qw(kg/s)	Qs(kg/s)	X
6	3.1	7.6	0.6
3	3.5	5.5	0.4
4	3.3	6.1	0.5
5	3.1	6.5	0.5
6	3.1	7.5	0.6

Flow Characteristics

Geothermal wells can be characterized by the mass flow and enthalpy of the steam-water mixture produced at various wellhead pressures. By plotting these characteristics, the general processes occurring in the reservoir can be inferred.

The well characteristic curves of LA-9D are shown in Fig 17, as entities the relationship between wellhead pressure and steam, water, total mass flow rate and fluid enthalpy extracted from the well. There were calculated and plotted using relatively stable data at different wellhead pressures. The wellhead pressure of LA-9D was 2.25 bar-g while using the 6-inch discharge pipe. It rose up to 11 bar-g when the 3-inch discharge pipe was used. Enthalpy increases at the decreasing of wellhead pressure: at 11 bar it is 1950kJ/kg and reaches 2153 kJ/kg at 2.65 bar. The steam flow rate is around 5.9 -8.0 kg/s for separation pressure of 1 bar but 5.5 to 7.6 kg/s with separation pressure 5 bar. The steam flow rate at 11 bars is around 6kg/s and 8 kg/s at 2.65 bar. The characteristic features of these data are the near-constant flowrate (mass flow) and the increasing enthalpy with decreasing wellhead pressure. The measurements show that the enthalpy of the fluid entering the well at low wellhead pressure is higher than at high wellhead pressures.

Such behaviour indicates that flashing occurs in the reservoir as a response to the pressure drop due to the mass extraction.

This fact is also confirmed by the shape of the curve of mass flow rate versus wellhead pressure, which is flat. Figure 17 shows that the flow rate does not increase much when the wellhead pressure decreases. This behaviour indicates that the well flow is choked because a lower receiver pressure (wellhead pressure) does not result in larger mass flow. In case of extraction of liquid phase only, the mass flow rate should increase at the decreasing of the wellhead, thanks to the higher pressure differential between reservoir, this effect of higher pressure differential is compensated by the lower relative permeability of steam with respect to water; therefore, mass flow rate does not increase significantly; the only increase occurs in the enthalpy. The curves are relatively flat, and the change of mass flow rate against the wellhead pressure is not large. The data at an early stage using 6-inch discharge pipe does not fit to the curve, and it is inferred that the discharge condition was not stabilised yet.

5.4 Discharge Testing of Well LA-10D

Figure 18 shows measurements during two flow tests in well LA-10D. The long term discharge test of LA-10D was started on 8 December 2015. The mass flow data was measured every hour during the testing period. The different size of discharge pipe with a diameter of 3”, 4”, 5” and 6” was used to obtain the stable discharge mass flow data at different wellhead pressure. The single well discharge test of LA-10D was completed up to 9 January 2016. The PTS logging was carried out on 21 March 2016 to obtain the data on flow condition in the wellbore. On 24 May, LA-10D was discharged again, and the discharge was completed on 15 June 2016.

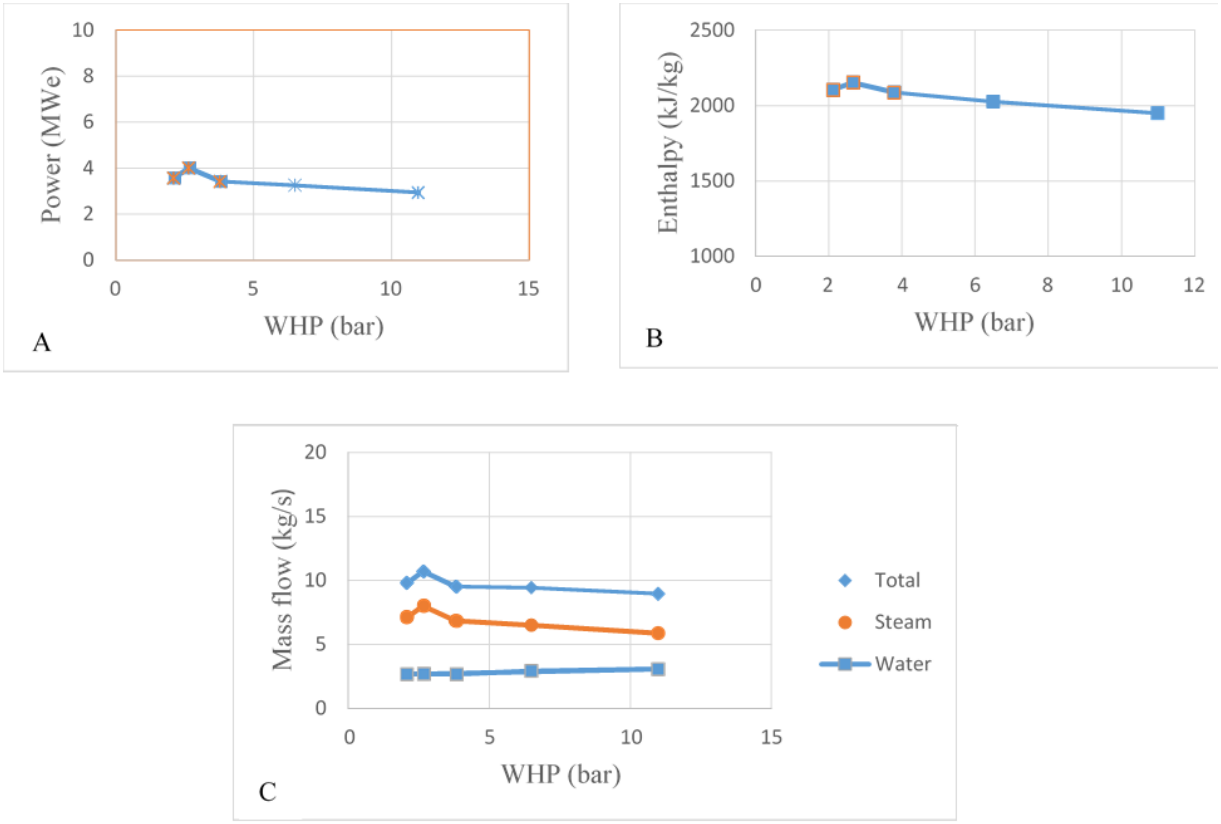

Figure 17: Characteristic curves of LA-9D, showing power (A), enthalpy (B) and mass flow rate (C) against wellhead pressure (WHP)

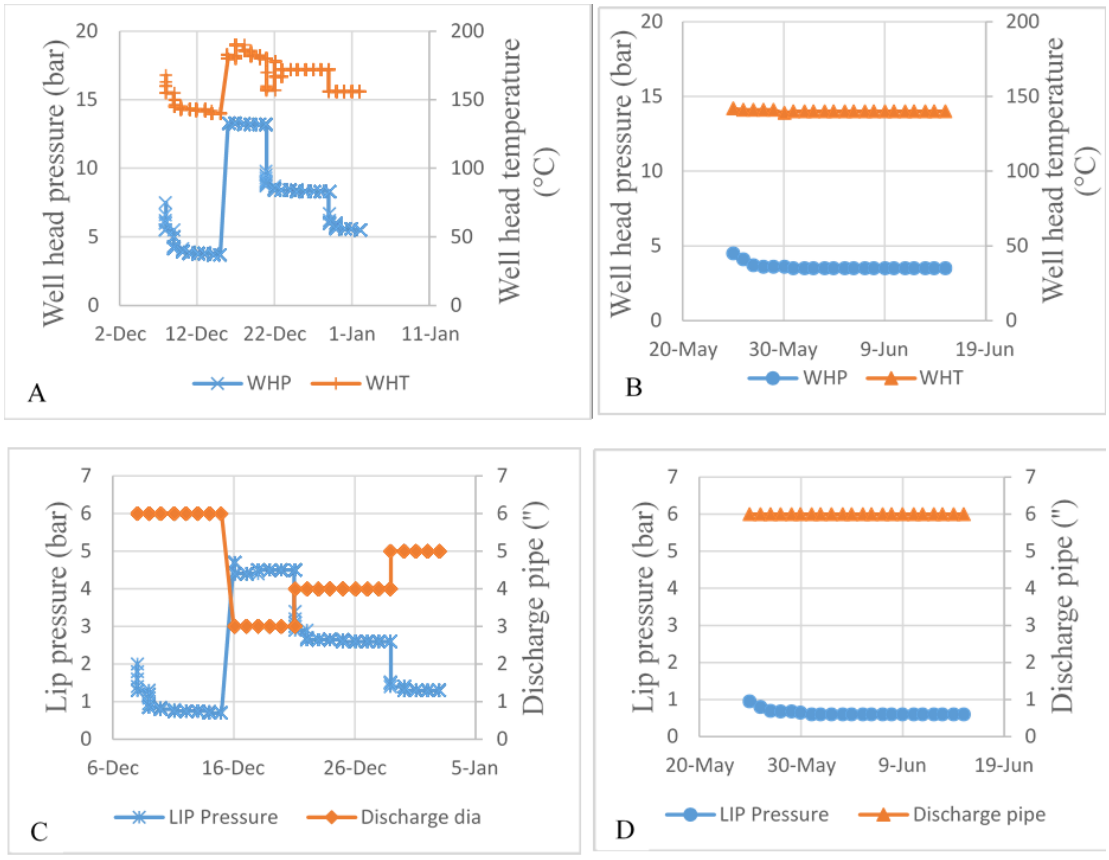

Figure 18: First (A and C) and Second (B and D) discharge test data of LA-10D, showing well head pressure and temperature (A and B) and lip pressure and discharge pipe diameter (B and D)

The PTS logging was tried on 14 and 15 of March 2016 at LA-10D while the well was discharging through 6" discharge pipe. However, the tool could not go deeper than 1040 m and 1113 m, respectively. On 21 March 2016, the sinker bar (weight bar) was connected to the tool, and then the tool could reach to close the well bottom. The wellhead pressure was 3.25 bar-g, and the total mass flow rate was 12.8 kg/s during the survey. The pressure, temperature, and spinner rotation data in the well were continuously measured and recorded from wellhead to around the well bottom with the PTS tool.

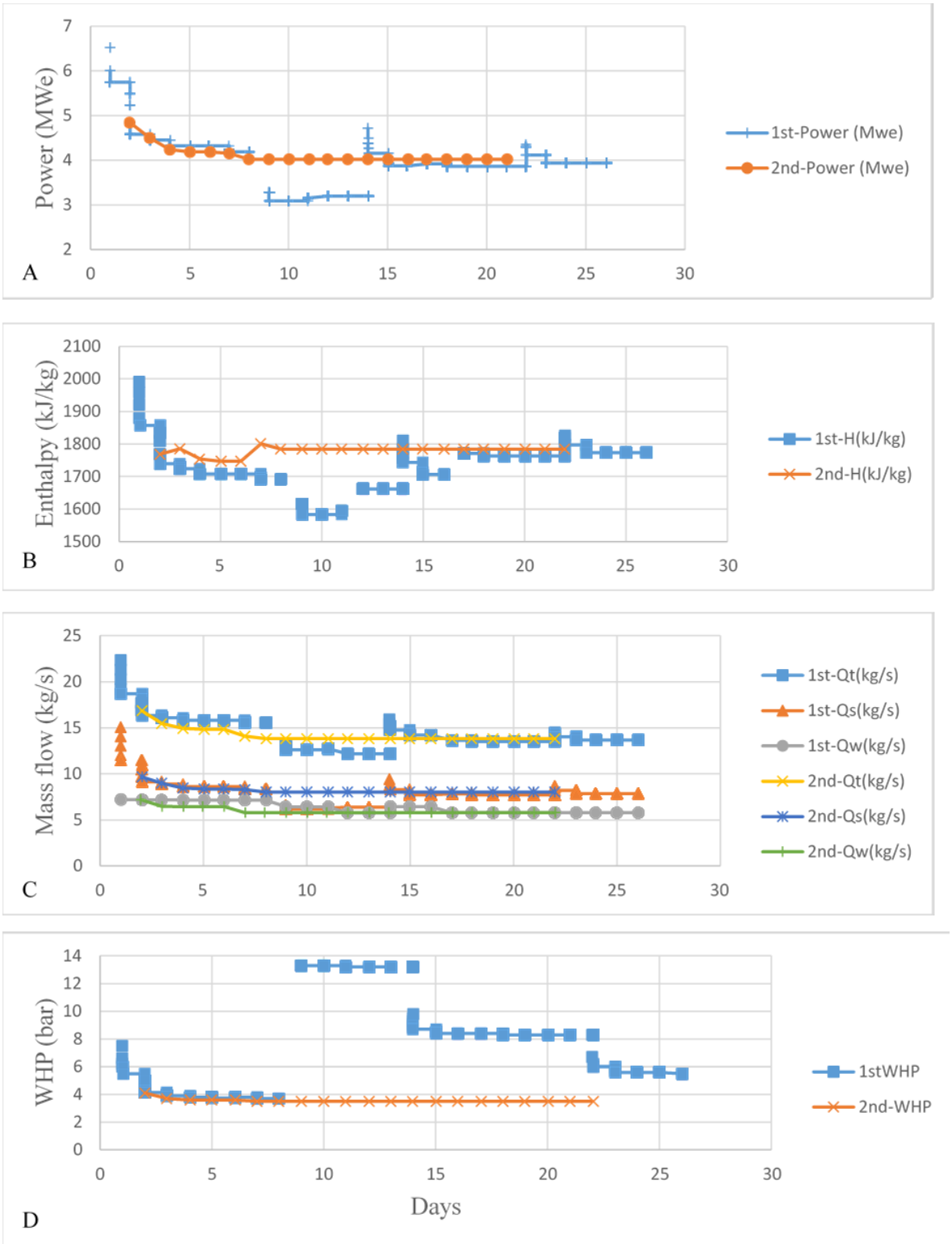

Figure 19: Results of first 30 days of LA-10D long term discharge test, after which it was constant (see Fig 18 B and D), showing wellhead pressure (D), flow rate (C), enthalpy (B) and power (A), in the calculated water, steam, total mass flow rate and fluid enthalpy of the first and second discharge test of LA-10D is shown in Table 11 and Fig 19. The first month is the period of single well discharge test, and the rest is the period of multi-well discharge test with well LA-9D. Different discharge pipe sizes were used in the test, and almost stable flow rates at each condition were obtained.

Biru

The analysis of the measurements from the single well discharge test of well LA-10D gives an estimate of steam flow in the range of 6.4 – 11.5 kg/s at the separation pressure of 1 bar-a which is equivalent to 3.2 – 5.7 MW electric power assuming 2 kg/s of steam flow converts to 1 MW_e. The steam flow rate at the wellhead pressure of 8.3 bar-g is 7.74 kg/s and 7.87 kg/s at a wellhead pressure of 5.6 bar-g. This is equivalent to 3.8 to 3.9 MW_e.

The 6-inch discharge pipe was used during the second test. The flow condition became stable, and the wellhead pressure and the total mass flow rate were constant at 3.5 bar-g and 13.83 kg/s.

The steam flow rate, the steam fraction was summarised in Table 12, and the equivalence of power (MWe) for 5 bar-a separation pressure is in the range of 2.9- 3.8 MWe.

Table 11: Measurements and results for well LA-10D from the Russel James lip pressure method with separation pressure of 1 bar-a

No	Date	P_0(bar)	P_c(bar)	D_p(inch)	W_{height}(cm)	H(kJ/kg)	Q_t(kg/s)	Q_w(kg/s)	Q_s(kg/s)	X
1	2015-12-15	3.7	0.7	6	12	1691.3	15.6	7.2	8.4	0.6
2	2015-12-21	13.2	4.5	3	11	1662.2	12.2	5.8	6.4	0.6
3	2015-12-29	8.3	2.6	4	11	1763.1	13.5	5.8	7.7	0.6
4	2016-01-05	5.6	1.3	5	11	1773.6	13.7	5.8	7.9	0.6
5	2016-04-01	3.3	0.5	6	10.5	1815.1	12.8	5.8	7.6	0.6
6	2016-06-15	3.5	0.6	6	11	1784.3	13.8	5.8	8.1	0.6

Table 12: Measurements and results for well LA-10D from the Russel James lip pressure method with separation pressure of 5 bar-a as in the Aluto-Lanagno pilot power plant

D_p (in)	Q_w(kg/s)	Q_s(kg/s)	X
6	7.9	7.6	0.5
3	6.4	5.8	0.5
4	6.4	7.1	0.5
5	6.4	7.2	
6	5.8	7	
6	6.5	7.4	0.5

The well characteristic curves of LA-10D shown in Fig 20, which shows the relationship between wellhead pressure and steam, water, total mass flow rate and fluid enthalpy extracted from the well, were plotted using relatively stable data at different wellhead pressure. The wellhead pressure of LA-10D was 3.25 – 3.7 bar-g while using the 6-inch discharge pipe. It rose up to 13. 2 bar-g when the 3-inch discharge pipe was used. The steam flow rate is around 6 -8 kg/s. The fluid enthalpy is 1662 – 1815 kJ/kg. The curves are relatively flat, and the change of mass flow rate against the wellhead pressure is not large. At the end of the first long term discharge test, the wellhead pressure was 3.25 bar-g, and the steam flow rate was 7.6 kg/s under the flowing condition with six-inch discharge pipe. The stabilised wellhead pressure and steam flow rate were 3.5 bar-g and 8.04 kg/s respectively during the second discharge.

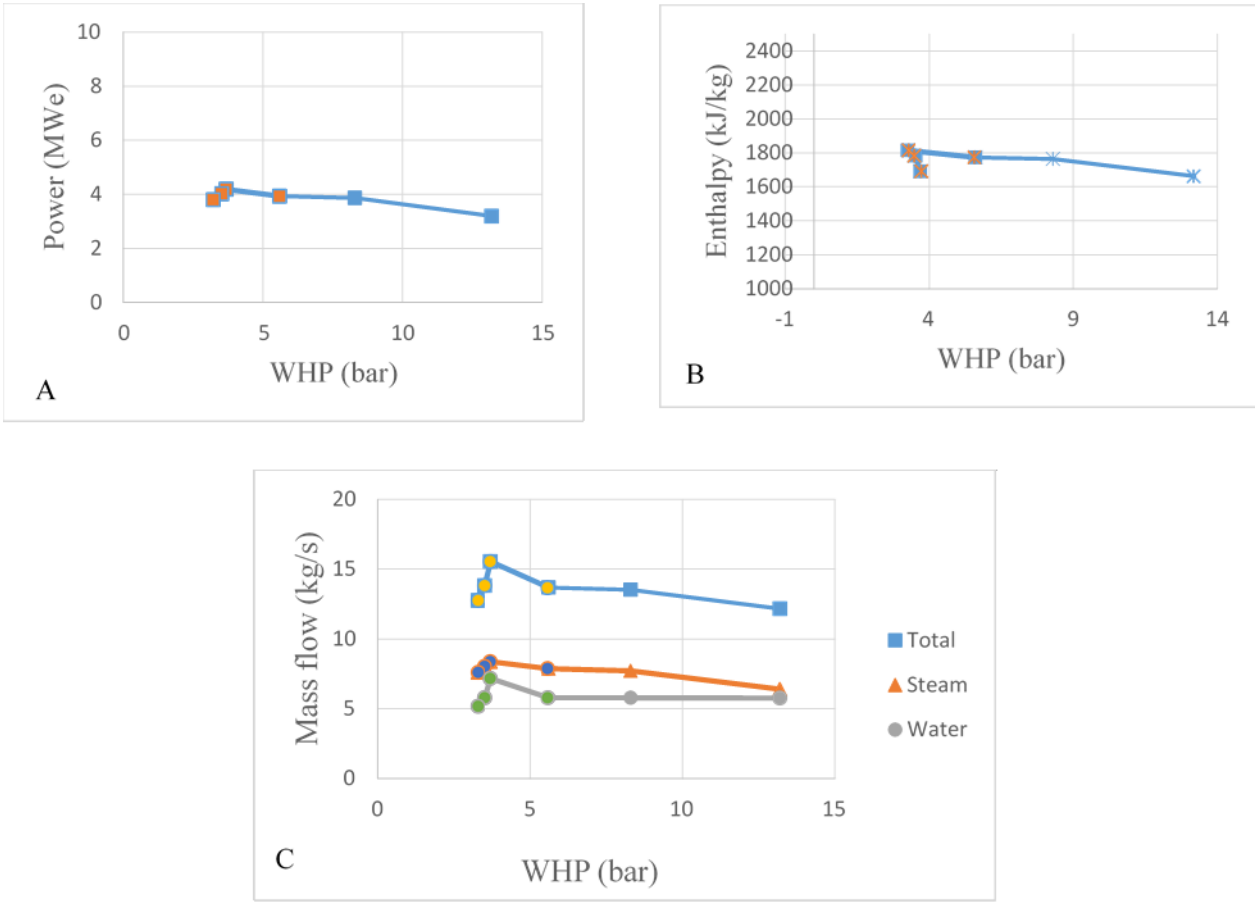

Figure 19: Characteristic curves of LA-10D, showing power (A), enthalpy (B) and mass flow rate (C) against wellhead pressure (WHP)

6. DISCUSSION AND CONCLUSION

The selected model for simulating the injection step tests in wells LA-3 and LA-10D assumed homogenous reservoir and constant boundary pressure. The results show in general better transmissivity in LA-10D than in well LA-3 and relatively good storativity in both of the wells. The transmissivity values were in the order of 10^{-9} [m^3/(Pa*s)] and 10^{-8}[m^3/(Pa*s)] for well LA-3 and LA-10D respectively and the storativity values in the order of 10^{-8} [m^3/(pa*m^2) or m/Pa] and they are classified as a liquid dominated geothermal reservoir.

The results for LA-3 of the skin factor for the best step show that it is -2.3 but in the range of -2.3 to -3.2 in the steps which had good simulations (CV criteria). These values indicate that the well has higher permeability in its closest surroundings than farther away and its effective radius is, therefore, larger than the real radius. The skin factor in the best step in LA-10D was on the other hand only -0.3 and in one step as high as 3.1, i.e. a positive skin factor, which means worse permeability in the close surroundings than farther away from the well.

The injectivity index is often used as a rough estimate of the connectivity of a well to the surrounding reservoir. Injectivity indices are fairly low for both wells, 1.1 (L/s/bar) for LA-3 and 1.6 (L/s/bar) for LA-10D.

Temperature and pressure data from LA-9D and LA-10D in the Aluto-Langano geothermal field were interpreted with the help of the Horner plot method to estimate formation temperature. The corresponding initial pressure of the reservoir was found using the Lip software. Results from LA-9D and LA-10D show an estimated formation temperature ranging from 300 to 311°C and 300 to 305 °C, respectively in the bottom of the wells. The pivot point of LA-9D is located at 1100 m vertical depth with the pressure of 85 bar. The pivot point of LA-10D is located at 1200 m vertical depth with the pressure of 92 bar. The Horner plot method did not prove equally useful in the interpretation of LA-10D as it did in the interpretation of LA-9D. Only three warm-up logs were available for LA-10D, and the first two only 12 hours apart, making the results from the interpretation more uncertain than in the case of LA-9D.

The analysis of the measurements from the single well discharge (first discharge) test of well LA-9D gives an estimate of steam flow in range of 5.4 – 7.6 kg/s at the separation pressure of 5 bar-a in Aluto-Langano pilot power plant which is equivalent to 2.7 – 3.8 MW_e of electric power output assuming 2 kg/s of steam flow convert to 1 MW_e.

The analysis of the measurements from the single well discharge test of well LA-10D gives an estimates of steam flow in range of 5.8 – 7.6 kg/s at the separation pressure of 5 bar-a in Aluto-Langano pilot power plant which is equivalent to 2.9 – 3.8 MW_e electric power assuming 2 kg/s of steam flow convert to 1 MW_e.

RECOMMENDATIONS

A major problem with these injection tests and all of the other injection tests performed on the Aluto-Langano wells lies in the test design. The time period for each of the steps is only about one hour. A better design is to let each injection step last at least three hours. In cases where the water supply is a problem, it is preferable to reduce the number of injection steps rather than their duration.

One or two steps of sufficient duration provide more useful results than ten steps that are too short. If the steps are long enough, they can all be analysed and produce good estimates.

It is important in new wells to measure temperature and pressure frequently during warm-up, especially at the beginning of the warm-up period for better interpretation of the formation temperature and initial pressure.

The importance of monitoring the wells through their lifetime should never be underestimated to be able to follow the evolution of the geothermal reservoir and the well themselves.

ACKNOWLEDGEMENTS

I want to express my deepest gratitude to the United Nations University, the Government of Iceland and the Ethiopian Electric Power (EEP) for allowing me to attend this training. I want to thank Mr. Ludvik S. Georgsson, director of the UNU geothermal training programme, Mr. Ingimar G.Haraldsson, deputy director for allowing me to study reservoir engineering, Ms Thorhildur Isberg, school manager, Mr Markus A.G. Wilde, service manager and Malfridur Omarsdottir, Environmental scientist and all staff of ISOR for the teachings, dedication to making us well educated.

My special thanks go to my supervisors, Dr Svanbjorg H. Haraldsdottir and Ms Saeunn Halldorsdottir, for sharing their great knowledge and experience, for their patience and support during this project. I would also like to thank Mr Kjartan Marteinsson for his support and guidance in using software developed in ISOR, and I want to thank former geothermal projects manager of EEP Mr Mulugeta Asaye for believing in me and allowing me to study in this study area.

Finally, I would like to thank my lovely wife, Sofia Midaso for having Sena, my newborn baby girl while I am doing this project.

REFERENCES

Arason, Th., Björnsson, G., Axelsson, G., Bjarnason, J.Ö., and Helgason, P., 2004: *The geothermal reservoir engineering software package ICEBOX, user´s manual*. Iceland GeoSurvey - ÍSOR, Reykjavík, report ISOR-2004/014, 80 pp.

Axelsson, G., 2012: The physics of geothermal energy. In: Saying, A., (ed.), *Comprehensive Renewable Energy, 7, 3-50.*

Axelsson, G., 2013: Geothermal well testing. *Paper presented at "Short Course V on Conceptual Modelling of Geothermal Systems"*, *UNU-GTP and LaGeo, Santa Tecla, El Salvador*, UNU-GTP, SC-17, 30 pp.

Bödvarsson, G.S., and Witherspoon, P.A., 1989: Geothermal reservoir engineering, part 1. *Geotherm. Scie & Tech, 2-1,* 1-68.

Bödvarsson, G.S., 1986: Independent review of reservoir engineering work at the Aluto-Langano geothermal field, Ethiopia. 10-12, 19-21.

ELC, 1986: Exploitation of Langano-Aluto geothermal resources, feasibility report. Electroconsult – ELC, Milan Italy, report.

Grant, M.A., and Bixley, P.F., 2011: *Geothermal reservoir engineering* (2nd ed.). Academic Press, Burlington, USA, 359 pp.

Haraldsdóttir S.H., 2016: *Well testing theory - injection.* UNU-GTP Iceland, unpublished lecture notes.

Helgason, P., 1993: Step by step guide to BERGHITI. User's guide. In: Arason, Th., Björnsson, G., Axelsson, G., Bjarnason, J.Ö., and Helgason, P., 2004: *ICEBOX – Geothermal reservoir engineering software for Windows, a user's manual*. Iceland GeoSurvey - ÍSOR, Reykjavík, report ISOR-2004/014, 80 pp.

Horne, R.N., 1995: *Modern well test analysis, a computer aided approach* (2nd ed.). Petroway Inc., USA, 257 pp.

Hutchison, W., Mather, T.A., Pyle, D.M., Biggs, J., and Yirgu, G., 2015: Structural controls on fluid pathways in an active rift system: a case study of the Aluto volcanic complex. *Geosphere, 11-3,* 542-562.

James R., 1970: Factors controlling borehole performance. *Geothermics, Sp. issue, 2-2,* 1502-1515.

Júliusson, E., Gretarsson, G.J., and Jónsson, P., 2008: WellTester 1.0b, user's guide. Iceland GeoSurvey - ÍSOR, Reykjavík, 27 pp.

Kebede, S., 2012: Geothermal exploration and development in Ethiopia: Status and future plan. *Paper presented at "Short Course VII on Exploration for Geothermal Resources", organized by UNU-GTP, KenGen and GDC, in Naivasha, Kenya*, UNU-GTP SC-15, 16 pp.

Marteinsson, K., 2016: *WellTester vs. 2, user´s manual*. ÍSOR – Iceland GeoSurvey, Reykjavik, report in publication.

Mohr, P., 1962: The Ethiopian Rift System. *Bull. Geophys. Obs. Addis Ababa, 5,* 33–62.

Steingrímsson, B., 2013: Geothermal well logging: Temperature and pressure logs. *Paper presented at "Short Course V on Conceptual Modelling of Geothermal Systems"*, *UNU-GTP and LaGeo, Santa Tecla, El Salvador*, UNU-GTP, SC-17, 16 pp.

Teklemariam, M., and Beyene, K., 2000: *Geochemical monitoring of the Aluto-Langano geothermal field, Ethiopia.* Geological Survey of Ethiopia, Addis Ababa, report., 13-15 pp.

Teklemariam, M., Battaglia, S., Gianelli, G., and Ruggieri, G., 1996: Hydrothermal alteration in the Aluto-Langano geothermal field, Ethiopia. *Geothermics, 25-6,* 679-702.

Teklemariam, M., 1996: Water-rock interaction processes in the Aluto-Langano geothermal field, Ethiopia. University of Pisa, Department of Earth Sciences, PhD thesis, 295 pp.

UNDP, 1986: Development of geothermal resources Ethiopia. UNDP, report, 6-7 pp.

WJEC, 2015: LA-9D well drilling report. West Japan Engineering Consultants, Inc, Tokyo Japan, report.

Worku Sisay, S., 2016. Sub-surface geology, hydrothermal alteration and 3D modelling of wells LA-9D and LA-10D in the Aluto-Langano geothermal field, Ethiopia. University of Iceland, Reykjavík, MSc thesis, UNU-GTP, report 7, 25-27 pp.